T.C.
IŞIK UNIVERSTIY
SCHOOL OF GRADUATE STUDIES

MASTER THESIS
DEPARTMENT OF ELECTRIC AND ELECTRONIC ENGINEERING
ELECTRONIC ENGINEERING PROGRAM

Ayça Burçak SARA

COGNITIVE DECISION INVESTIGATION WITH COMBINED EEG GAMMA OSCILLATIONS AND EYE-TRACKING (EOG)

SUPERVISOR
Assists. Prof. Dr. Rüştü Murat DEMİRER

İSTANBUL, September 2024

T.C.
IŞIK UNIVERSITY
SCHOOL OF GRADUATE STUDIES

MASTER THESIS
DEPARTMENT OF ELECTRICAL AND ELECTRONIC ENGINEERING
ELECTRONIC ENGINEERING PROGRAM

Ayça Burçak SARA

(21ELEC5008)

COGNITIVE DECISION INVESTIGATION WITH COMBINED EEG GAMMA OSCILLATIONS AND EYE-TRACKING (EOG)

SUPERVISOR

Assists. Prof. Dr. Rüştü Murat DEMİRER

İSTANBUL, September 2024

T.C.
IŞIK UNIVERSITY
SCHOOL OF GRADUATE STUDIES

MASTER THESIS
DEPARTMENT OF ELECTRICAL AND ELECTRONIC ENGINEERING
ELECTRONIC ENGINEERING PROGRAM

Ayça Burçak SARA

(21ELEC5008)

COGNITIVE DECISION INVESTIGATION WITH COMBINED EEG GAMMA OSCILLATIONS AND EYE-TRACKING (EOG)

Date: 13.09.2024

Thesis Supervisor:
Assist. Prof. Dr. Rüştü Murat DEMIRER / Işık University
Jury Members:
Assoc. Prof. Dr. Burcu TUNGA / İstanbul Technical University
Assist. Prof. Dr. Ayşenur GÜL / Işık University

İSTANBUL, September 2024

ABSTRACT

COGNITIVE DECISION INVESTIGATION WITH COMBINED EEG GAMMA OSCILLATIONS AND EYE-TRACKING (EOG)

With the progress in technology, the integration of neuroscience and sensory has assumed a very crucial role in discovering or unraveling cognitive functions. This thesis explores how EEG gamma oscillations and EOG eye tracking signals relate to cognitive decisions. Cognitive decision making, which encompasses attention, memory, and problem-solving abilities, is inherent in human functioning and hence grasping cognition enhances several fields including psychology, neuroscience, decision-making theories, among others.

The study builds on the EEGEyeNet dataset to understand the coupling between the EEG activity and eye movements in decision making tasks, for 356 subjects in total. The contribution of high frequency gamma oscillations to saccadic eye movements is therefore investigated using additional EEG and EOG analysis techniques such as CPSD and phase space analysis. The findings clearly show that at a lower frequency band, the results are partially in line with the assumption that EEG and EOG activity is partially coordinated to the extent of decision-making task, while at high frequency bands, the EEG and EOG signals are partially asynchronous. This could suggest that this independence is the result of dissociated cognitive and neural substrates that control brain function and eye motion during processes that involve decision-making. The overall conclusions of this thesis help to advance the knowledge of how EEG and EOG signals can be combined for the investigation of cognitive decision-making processes. The study equally provides evidence towards the pliability and possibility of integrating these together for analysis of the neurological drivers of decision making while at the same time creating further

research suggestions grounded on the accomplishment of achieving a blend of multiple physiological data feeds. Which could in turn bring about better cognitive models and better methods of rectifying poor decision making. It is hoped that this study will serve as a useful resource for other scholars from cognitive psychology, neuroscience, and human computer interaction where it may help advance studies on brain processes related to eye movement and decision making.

Keywords: EEG, EOG, Cognitive Decision-Making, Gamma Oscillations, Eye-Tracking

ÖZET

BÜTÜNLEŞİK EEG GAMA SALINIMLARI VE GÖZ TAKİBİ (EOG) İLE BİLİŞSEL KARAR ARAŞTIRMASI

Teknolojideki ilerlemeyle birlikte, nörobilim ve duyusalın entegrasyonu bilişsel işlevleri keşfetmede veya çözmede çok önemli bir rol üstlenmiştir. Bu tez, EEG gama salınımlarının ve EOG göz izleme sinyallerinin bilişsel kararlarla nasıl ilişkili olduğunu araştırmaktadır. Dikkat, hafıza ve problem çözme yeteneklerini kapsayan bilişsel karar verme, insan işleyişinin doğasında vardır ve bu nedenle bilişi kavramak psikoloji, nörobilim, karar verme teorileri gibi çeşitli alanları geliştirir.

Çalışma, toplamda 356 denek için karar verme görevlerinde EEG aktivitesi ve göz hareketleri arasındaki bağlantıyı anlamak için EEGEyeNet veri setine dayanmaktadır. Bu nedenle, yüksek frekanslı gama salınımlarının sakkadik göz hareketlerine katkısı CPSD ve faz uzayı analizi gibi ek EEG ve EOG analiz teknikleri kullanılarak araştırılmaktadır. Bulgular, daha düşük frekans bantlarında sonuçların, EEG ve EOG aktivitesinin karar alma görevinin kapsamına göre kısmen koordineli olduğu varsayımıyla kısmen uyumlu olduğunu, yüksek frekans bantlarında ise EEG ve EOG sinyallerinin kısmen asenkron olduğunu açıkça göstermektedir. Bu, bu bağımsızlığın, karar almayı içeren süreçler sırasında beyin fonksiyonunu ve göz hareketini kontrol eden ayrışmış bilişsel ve sinirsel alt tabakaların sonucu olduğunu düşündürebilir.

Bu tezin genel sonuçları, EEG ve EOG sinyallerinin bilişsel karar alma süreçlerinin araştırılması için nasıl birleştirilebileceğine dair bilginin ilerlemesine yardımcı olur. Çalışma, karar almanın nörolojik itici güçlerinin analizi için bunların bir araya getirilmesinin esnekliği ve olasılığına yönelik kanıtlar sunarken, aynı zamanda birden fazla fizyolojik veri beslemesinin bir karışımını elde etme başarısına dayanan daha fazla araştırma önerisi oluşturur.

Bu da daha iyi bilişsel modeller ve zayıf karar vermeyi düzeltmenin daha iyi yöntemlerini ortaya çıkarabilir. Bu çalışmanın bilişsel psikoloji, sinirbilim ve insan bilgisayar etkileşimi alanındaki diğer bilim insanları için yararlı bir kaynak olarak hizmet etmesi ve göz hareketi ve karar vermeyle ilgili beyin süreçleri üzerine yapılan çalışmaları ilerletmeye yardımcı olması umulmaktadır.
Anahtar kelimeler: EEG, EOG, Bilişsel Karar Verme, Gama Salınımları, Göz Takibi

ACKNOWLEDGEMENT

First, I want to extend my heartfelt thanks and appreciation to my supervisor Dr. Rüştü Murat Demirer for giving his valuable time and for his encouragement and support during this research. He has indeed provided me with his expertise as well as his input in this thesis and has encouraged me to endure even during the toughest times.

I would like to especially thank my family and friends as they never only encouraged me to develop my studies as their priority but also supported me in different ways as the endeavor needed time and energy. Their cheerful outlook towards me and confidence in my capacity has been quite inspiring, especially when things were hard during this process.

I also would like to thank the participants in this study as without their participation in this study their time and effort this research could not have been done. Also, I express my appreciation to the authors and developers of the EEGEyeNet dataset that was widely used to develop this work.

Finally, I am grateful to all the individuals and institutions which helped me in preparing this thesis and giving a part of their valuable time to me.

Ayça Burçak SARA

This thesis is dedicated to my mother and sister for their endless love and support. Their belief in my potential fueled my determination to complete this project.

TABLE OF CONTENTS

LIST OF FIGURES

ABBREVIATIONS LIST

EEG: Electroencephalogram

EOG: Electrooculogram

CPSD: Cross Power Spectral Density

MSC: Magnitude Squared Coherence

MSCA-MI: Magnitude Squared Coherence Analysis – PAC

MI: Phase-Amplitude Coupling

FT: Fourier Transform

DFT: Discrete Fourier Transform

CHAPTER 1

1. INTRODUCTION

The main purpose of the study is to investigate the effect of the EEG gamma oscillations and eye tracking (EOG) on the cognitive decision-making process. The process of cognitive decision making determines human's daily life activity in many different situations and affects their behavior. These processes contain all types of decision-making that humans make during their daily life.

EEG gamma oscillations and eye tracking are the most powerful tools to observe cognitive decision-making processes. The high frequency oscillation in the brain associated with the cognitive process is EEG gamma oscillations and they provide a high-time resolution measure of brain activity.

The study aims to provide a detailed model that can help us to understand the EEG and eye-tracking effect on the cognitive decision-making process. Also with this study, contribution to cognitive psychology, neuroscience and decision-making theory is aimed. The investigated studies and findings can explain the main mechanism under the decision-making process and be a basis for future work in this field.

1.1. RESEARCH OBJECTIVES

The analysis of change in the electrical patterns of the brain during the several stages of the choice-making processes will be made by using EEG. It will also help in establishing the areas of the brain that aid in decision-making and the neurology interactively implicated.

The eye-tracking technique was chosen to make more sensitive and more concrete data, and it is determined to which objects participants' eyes are turning during the decision-making process and in what order. This will be done to show

that attention and perception, especially the kind that focuses on the visual impact influence decisions.

The knowledge gap in the decision-making process will be addressed by the present study which intends to ascertain the role of neurophysiological and visual inputs for decision making by synchronously acquiring EEG & Eye-tracking data. This will lead to the capturing of a wider picture of the decision-making processes since both the eye and head movements will be monitored at the same time comprehending the movement and decision-making patterns.

1.2. IMPORTANCE OF RESEARCH

This study will help develop a link between the neurophysiological and the visual areas of the mind involved in decision making and will contribute valuable information to current data sources on it. This way of combining both EEG data and eye-tracking data will contribute to the development of enhanced knowledge regarding the decision-making processes and the enlargement of theoretical models of these processes as well.

1.3. GUIDANCE FOR FUTURE RESEARCH

By showing the potential of using both EEG and eye-tracking technologies, this study sets a path for future studies. It would be important to provide more insight into neurophysiological and visual factors underpinning decision-making mechanisms through further studies in this area. On the other hand, fresh leads arising from integration of these devices will open doors for multidisciplinary research.

The combination of EEG gamma oscillation and eye-tracking systems, new analysis methods and techniques can be developed and the examination on decision-making process can be more sensitive and detailed.

1.4. THESIS STRUCTURE

The thesis will start by giving the general objective and importance of the topic and its guidance to future research. Then it will continue with the general information that needs to be known to understand the analysis and discussion on the topic. After that the methodology to obtain and analysis the data will be given. At the end, the analysis results will be investigated in the result section and the discussion part will summarize all the findings and implementation of the thesis topic.

1.5. BACKGROUND AND MOTIVATION

The decision-making of humans plays an important role in the daily undertakings of humans, it involves and influences several decisions in the lives of humans. Thus, realizing these processes, it becomes much simpler to make correct and realistic choices on the same note, one gets an opportunity to realize the importance of decision-making throughout his or her daily life and multifaceted vocations inclusive of business and marketing, education, and health, among others. But within the last few years, because of the discoveries of neurophysiology and cognitional sciences, the neurophysiology of decision-making is addressed to some extent. In this respect, the Electroencephalography (EEG), and eye-tracking method are the most used approaches in decision-making.

CHAPTER 2

2. LITERATURE SURVEY

2.1. COMBINING EEG AND EYE TRACKING

Widely emphasized problem of eye movement artifacts in the electroencephalographic (EEG) data is discussed by Plöchl et al. (2012) reveal a new concept for eliminating this problem. Saccades, blinks, and micro-saccades are eye movements that impose considerable noise to EEG that might either veil or distort neural activity. More traditional approaches include linear regression, and independent component analysis (ICA), which have been used with a certain level of success; however, this is still problematic due to the multifaceted and interfering nature of most of these artifacts.

In the present study, the authors employed both EEG and eye-tracking data from participants that were asked to perform guided eye movement tasks. They provided a careful analysis of the properties of multiple types of eye movement artifacts including corneo-retinal dipole shift, saccade spike potentials, and those generated by the eyelid and clarified its peculiarity of each and their effect on EEG, respectively. Their results extend previous research showing that such artifacts stem from independent sources and, therefore, correction procedures may need to be beyond a one-size-fits-all approach.

Another strength of this work is to compare various types of artifact correction procedures. The authors indicated that most of the regression-based approaches end up over correcting or under correcting the EEG data based on the electrode site as well as nature of the eye movement. On the other hand, in the case of ICA, there was shown a higher capacity to Cancel them since, thanks to the independence of the sources of artifacts, this approach allows avoiding the influence of interferences on the signals. On the other hand, certain issues

emerge while using ICA, for instance, to differentiate between artifacts originating from the eyes as well as pertinent neural signals in the absence of other data.

In an effort to improve the robustness and the level of automation of the correction of artifact ICA components, the authors put forward an eye tracker-based algorithm that aims to determine the set of eye-movement-related ICA components. This algorithm was also seen to take the correct decisions at par with the human experts in case it was endowed with both IC topographies and activations and in case the information given was limited to only the IC topographies; the algorithm was seen to perform far superior to the experts. Receiver operated characteristic analysis added more credibility to the algorithm proving that the algorithm has the best precise value of false negatives and false positives.

The relevance of this work can be seen in the areas of cognitive neuroscience and clinical research as EEG is employed in both lines of studies. Higher accuracy in artifact correction thus results in increased accuracy of the interpretations of the neural data, especially in the paradigms linked to overt attention and naturalistic viewing conditions. The study also provides researchers with directions toward exploring ways of enhancing further automated artifact correction processes, while maintaining the EEG data quality despite the inevitable eye movements.

Altogether, Plöchl et al. (2012) are useful for researchers, who work with the EEG data containing eye movements artifacts. Their systematic analysis and the subsequent solutions presented can be viewed as a progressive contribution to the never-ending task of enhancing the quality of the EEG signal and, as a result, the reliability of the tests aimed at evaluating cognitive and neurological functioning.

2.2. THE PERIPHERAL PREVIEW EFFECT WITH FACES

In a study published in Neuropsychologia, Huber-Huber et al. (2019) examine the processes of visual stability during saccade using a technique of EEG and eye-tracking. The current study mainly concentrates on the peripheral preview effect that entails the use of peripheral information acquired prior to the time the eye shifts to focus on a particular object in face stimuli. Saccades are sudden movements of the eyes and when predicting the effects of saccades on vision, the authors examine if various sensory conditions involve preview processes that are helpful to envision stability.

The work consisted of two experiments performed with subjects who were instructed to look at target faces at the periphery. These stimuli either retained the orientation in which the preview was made (valid preview) or altered the orientation in a saccade (invalid preview). Eye displacement was quantified by comparing the participants' performance in discriminating the face orientation post-saccade and the EEG data were further analyzed to provide an insight on how various phases of trans-saccadic processing occur in a temporal manner.

Preliminary outcomes of the study are as follows: it is established that the increase of the post-saccadic discrimination performance is conditioned by valid preview; the fixation-locked N170, which is known as the face-specific component, has been reduced. This reduction indicates that there are benefits for the integration of pre-saccadic and post-saccadic information for fast categorization of the target face. Furthermore, the study highlights that trans-saccadic visual stability may involve multiple temporal stages: prediction of the saccadic target, integration of pre- and post-saccadic information within a few hundred milliseconds of the onset of fixation and helps in rapid categorization based on the integrated information.

The preview effect was also studied by Huber-Huber et al. (2019) when they investigated the impact of task context on the ability when varying the proportion of valid and invalid trials. An important thing to note is that the preview effect was discovered to be rather consistent and thus not greatly

dependent on context-based prediction. Yet, the researchers found that pre saccadic expectations enhance the EEG response during the period that precedes the saccade hence it was seen that there were some form of predictive processing that could affect how visual information is processed across saccades.

This work is a valuable addition to the knowledge of how the brain preserves image steadiness while saccadic eye movements constantly interrupt this process. Indeed, in proving that the brain implements predictive systems and amalgamates visual data across saccades, this analysis contributes toward the enhancement of the theoretical construct of trans-saccadic vision. It also provides methodological implications for possible future research on how EEG and eye-tracking can be integrated to investigate processes as to visual predictiveness and steadiness.

2.3. INVESTIGATION OF TASK-SWITCHING WITH SIMULTANEOUS EEG AND EYE-TRACKING

The study seeks to establish whether the functions related to performance of the two tasks are sequential or simultaneous, hence the following question based of the study by Longman et al. (2021): It is therefore based on the task-switching paradigms where the participants are supposed to perform two or more tasks, which call for a change in task-set parameters including the perceptual and response selection. The authors analyze temporal properties of this reconfiguration by means of electroencephalography (EEG) and eye-tracking.

In the given study, the participants categorized the digits displayed at the same time and each digit-accompanied task had a specific semantic affinity to the digit. The findings of the presented study were meant to shed light upon the highly important question whether the preparatory processes associated with the positivity in the EEG and anticipatory orientation of gaze are organized in parallel or not, and, if this is so, in which manner. The presented results indicated that EEG positivity is usually present after and locked in time to anticipatory fixation on the task area, thus, implying a serial organization. But, this seriality

was not perfectly marked; in trials with early fixations, the positivity was earlier over the cue onset relative to fixation suggesting a more parallel processing in some aspects of task-set reconfiguration.

The findings of this study are important for unraveling how the brain is able to regulate cognitive control when multitasking. The results indicate that the reconfiguration of task-set components cannot be entirely sequential and may involve parallel processes that can also have different temporal patterns concerning task and time requirements. This goes against the assumptions of conventional theories of task-set reconfiguration that call for a sequential approach to reconfiguration and supports the need for a theory that captures both sequential and simultaneous ways of reconfiguration.

In their study published in Nature Human Behavior , Longman et al. (2021) add to the previous debates on cognitive control by finding new evidence against the method of task-set reconfiguration. Concurrent EEG and eye-tracking methods are extremely valuable for studying cognitive processes' time dynamics and is critical for constructing more accurate models of cognitive control in multitasking conditions.

CHAPTER 3

3. GENERAL INFORMATION & METHODOLOGY

3.1. GENERAL INFORMATION

3.1.1. Signal Processing

Signal processing has become an integral aspect of electrical engineering as well as applied mathematics focusing on analyzing, changing, and understanding different types of signals. The signals can either vary with time or location depending on their nature; they can be sound waves, light waves, or radio waves while biological signals like EEG and ECG also fall into this category. Processing of signals is another area broadly defined and aimed at improving, minimizing, or obtaining valuable information from signals with the use in countless applications from communication systems to biomedical diagnostics.

Analog and Digital signal processing continue to be closely related with each other and are two similar signals.

Signal processing can be simply classified in two fields: the analog field and the digital field. Analog signal processing processes is processing signals in their analog form using techniques such as filtering, modulation, and amplification among others to preserve signal quality (Oppenheim & Schafer, 2009). This form of processing has appeared to be relevant in the establishment of communication methods such as radio and television (Smith, 1997).

Digital Signal Processing (DSP), however, deals with signals after these are converted from analog to digital form. Digital techniques are preferred because these form functional techniques because they are flexible, accurate and are capable of handling complex algorithms as compared to analog techniques (Proakis & Manolakis, 2007). DSP covers various methods such as filtering that

involves different types of filters like butter words and Chebyshev types; transformation comprises of Fourier and wavelet transformations; and compression that include many algorithms such as the AM radio and a lot of other applications involve audio and speech, image, and video processing etc.

3.1.1.1. Filter Characteristic

Filters perform the function of eliminating unwanted parts of signals, picking out the required portions as well as improving the quality of the whole signal. The characteristics of filters include:

Passband: A range of frequencies that is accommodated by the filter with the associated tolerance being high;

Stopband: A range of frequencies that is stated to be reduced in a great manner by some filters.

Cut-off Frequency: This is defined as the frequency point where the passband transforms into stopband and a further addition does not make a change.

Roll-off rate: The roll-off rate refers to the response of the filter to a signal that has exceeded the value of the cut-off frequency.

Ripple: This means measuring the variation lying between the response to amplitude within the passband (passband ripple) or the stopband (stopband ripple).

These characteristics are very crucial when it comes to synthesizing filters for a wide range of applications (Oppenheim & Schafer, 2009).

The common filters that are used and their mathematical expressions are given below.

Butterworth Filter: The ideal filter that requires a smooth frequency response by characterized maximally flat response in the passband without ripples. The formula of the n-th order transfer function for Butterworth filter is:

$$\boldsymbol{H(s) = \frac{1}{\sqrt{1 + \left(\frac{s}{\omega_c}\right)^{2n}}}} \tag{3-1}$$

where the complex frequency is $s = j\omega$, angular frequency cutoff is ω_c and filter order is n (Proakis & Manolakis, 2007).

Chebyshev Filter: It has a sharper roll-off compared to the Butterworth filter but at the expense of ripples in either the passband (Type I) or stopband (Type II).

$$\boldsymbol{H(s) = \frac{1}{\sqrt{1 + \epsilon^2 T_n^2\left(\frac{s}{\omega_c}\right)}}} \tag{3-2}$$

where ripple magnitude controlled by ϵ, the Chebyshev polynomial is T_n (Oppenheim & Schafer, 2009).

3.1.1.2. Fourier Transform

The Fourier Transform (FT) is a critical, mathematical, tool in Signal processing; the FT converts a signal in the time domain to its frequency domain. The FT of a continuous time signal x(t) is defined as in below indicates where X(f), is the frequency domain description of the signal x(t) - in addition, f is the frequency variable.

$$\boldsymbol{X(f) = \int_{-\infty}^{\infty} x(t) e^{-j2\pi ft}\, dt} \tag{3-3}$$

FT's uniquely allow for the expression of a signal in its constituent frequencies; this is especially useful for any application that requires frequency decomposition, such as audio and speech processing, image processing, and use in the Biomedical signal processing systems (Oppenheim & Schafer, 2009).

The Discrete Fourier Transform (DFT) of Digital are typically Computationally efficient to calculate with the Fast Fourier Transform (Cooley & Tukey, 1965).

3.1.1.3. Wavelet Transform

The Wavelet Transform (WT) is an elegant, effective, and theoretically sound mathematical framework developed in signal processing for multi-scale and multi-resolution analysis and representation of signals. In contrast to the

Fourier Transform, which analyzes and represents signals based on their frequency content without accounting for time localization, the Wavelet Transform has both time and frequency localization. Therefore, the WT is particularly effective for signal analysis when the frequency content changes over time, such as for biomedical signals, speech, and images (Mallat & Peyré, 2009).

The Wavelet Transform decomposes a signal into a set of basic functions called wavelets, where wavelets are generated from a single prototype wavelet by dilations (scaling) and translations (shifting). This means the WT uses multiresolution analysis represented in both the coarse-grained and fine-grained scales, meaning the WT is effective for detecting waveforms and discerning their transient features (Addison, 2017). There are two main types of wavelet transformation.

Continuous Wavelet Transform (CWT): A situation where the signal is viewed as a function over "time" and "scale" and provides a continuous mathematical representation of the signal x(t).

$$\boldsymbol{W_x(a,b) = \int_{-\infty}^{\infty} x(t)\psi^*\left(\frac{t-b}{a}\right)dt} \tag{3-4}$$

where $W_x(a,b)$ is the wavelet coefficient at scale a and position b, original signal is $x(t)$, mother wavelet which is a function that localized in both time and frequency is $\psi(t)$, $\psi^*(t)$ denotes the complex conjugate of the mother wavelet.

The CWT provide a detailed representation of signals time frequency characteristics over a range of scales and position (Mallat & Peyré, 2009)..

Discrete Wavelet Transform (DWT): A situation where the signal is viewed as a function over specific scale and time points and provides a discrete mathematical representation of the signal. The DWT is used in practice due to its computational speed.

$$\boldsymbol{W_{j,k} = \sum_{n=-\infty}^{\infty} x[n]\psi_{j,k}^*[n]} \tag{3-5}$$

where $W_{j,k}$ are the wavelet coefficients ad discrete scale j and position k, $x[n]$ is the discrete signal, $\psi_{j,k}[n]$ is the discrete wavelet which is generated by scaling and translating the mother wavelet.

By successfully dividing down the signal into several resolution levels, the DWT can capture both low-frequency trends and high-frequency details (Kovacevic & Vetterli, 1995; Proakis & Manolakis, 2007).

3.1.1.4. Biomedical Signal Processing

Signal processing applications to biomedical signals is widely applied in biomedical applications. Digital filters plays a curial role in the physiological signal processing helps to reduce noise, artifact reduction and enhancing features to enhance features for the purpose of diagnosis. Band-pass filters are often applied to EEG signals to extract specific frequency bands corresponding to various activities of the brain (Cohen & Cuffin, 1983). Wavelet transform approaches further advanced the outcomes in terms of non-stationary biomedical signals permitting both time and frequency localization, which is important when detecting and classifying medical conditions (Addison, 2017). Conclusion Signal processing remains an important technology that supports many modern applications across several disciplines, including telecommunications and healthcare. The advances of the digital signal techniques (e.g., Fourier and Wavelet transforms) and different forms of filters (e.g., digital filters) have contributed to more effective and accurate signal representations.

3.1.2. Biomedical Signals

Biomedical signals are signals used to obtain information by observing the physiological activities of a biological system or organs. This information gathering can be as simple as a doctor estimating a patient's blood pressure by feeling the patient's heartbeat with his or her fingers, or as complex as performing tissue analyses of internal organs using computed tomography (Bronzino, 2000).

Biomedical signals can be classified according to their physical sources, application areas and characteristics. Classifying signals according to their characteristics is more important from an analytical point of view. Because the techniques used in signal processing do not change according to the other two rounds of classification, i.e., signal source or application area (such as cardiology, neurology). In this context, general information about classification according to physical sources will be given rather than classification according to application area (Bronzino, 2000; Özdamar, 2009). According to their physical sources, biomedical signals are classified as follows (Bronzino, 2000).

Bioelectric Signaling: Bioelectric signals are recognized as the most important biomedical signals. These signals are generated by nerve and muscle cells and have unique properties. In other words, the bioelectric signal of each biological system is different. The source of bioelectric signals is cell membrane potential, which generates action potential when appropriate conditions are provided. The action potential is formed by the differentiation of the ion density in the cell membrane and the opening and closing of the cell membrane. Depending on the research, it may be necessary to measure bioelectrical signals generated by a single cell or by a community of cells. In single cell measurements, microelectrodes are used as receivers and the bioelectrical signal measured in this case is the action potential generated in the cell. In more complex systems, different electrodes need to be used for measurement. In this case, the bioelectric signals generated by many cells are measured by sensors. Apart from cellular research, bioelectric signals are measured not at the point of generation, but when they pass through various organs and reach the surface (Bronzino, 2000).

Examples of bioelectrical signals include electroencephalogram (EEG), which is electrical signal measured through the skull, electrocardiogram (ECG), which are heart rhythms measurements, electromyogram (EMG), which occurs in muscles, electroretinogram (ERG), which is obtained from the retina and is used to determine the visual field, and electrooculogram (EOG) of eye movements (Bronzino, 2000).

Bioimpedance Signaling: The impedance of an organic tissue contains many biological information such as some components of that tissue; the volume and distribution of blood passing through it, hormonal and automatic nervous system activation. Bioimpedance signals are obtained by sending sine currents in the range of 50kHz-1Mhz frequency and 20μA - 20mA voltage range to the tissues for testing purposes (Bronzino, 2000).

Bioacoustics Signaling: The noise created by the blood during the flow of blood through the heart valves and veins or the sounds made by the air as it passes between the upper and lower airways in the lungs (such as coughing, snoring, chest, and lung sounds) are called bioacoustics signals (Bronzino, 2000).

Bio-magnetic Signals: Organs such as the brain, heart and lungs generate very weak magnetic fields. Measurement of the signals generated by these organs helps to obtain information that cannot be obtained from other biomedical signals (Bronzino, 2000).

Biochemical Signaling: Biochemical signals are usually exceptionally low frequency signals obtained because of chemical measurements on living tissue or samples analyzed in the laboratory (Bronzino, 2000).

Bio-optic Signals: Bio-optical signals are signals generated because of optical activities in a biological system. By sending different wavelengths of light to an organ, oxygen levels in that organ can be estimated by measuring the light transmitted and reflected by the organ. Valuable information about the fetus can be obtained by measuring the heating structure of the amniotic fluid. By introducing a colored substance into the circulatory system, the condition of the heart can be estimated. Especially the development of fiber optic technology has contributed to the application areas of bio-optical signals. The relative signal processing characteristic categorization of biomedical signals is the one that best facilitates signal classification. The details of signal processing techniques are different than their origin and applications of signal instead they are categorized by the types of signals they deal with (Bronzino, 2000).

3.1.3. Electroencephalogram

EEG is another common technique of neuroimaging that records the electric activity of the neurons which arise due to firing. The EEG records potential generated by the ionic currents in neurons of the brain together with a voltage. It mainly records from structures of the cerebral cortex, especially the pyramidal neurons owing to their structural arrangement and orientation which is perpendicular to the surface cortex and hence allows the summation of electrical activity that can be recorded by scalp electrodes (Niedermeyer, E., Da Silva, F. L., et.al., 2004).

EEG is an invasive process that covers high temporal resolution of approximately milliseconds, implies the appreciation of rapid fluctuations in the brain activity, which may take place in cognitive or in the case of epilepsy activities. However, its spatial resolution is worse than most neuroimaging methods, such as functional magnetic resonance imaging (fMRI), because of signal attenuation by the skull and scalp.

3.1.3.1. Anatomy and Physiology of the Brain

The human brain is a complex organ composed of approximately 86 billion neurons, responsible for a wide range of functions including cognition, sensation, and movement. It is divided into several key areas that each contribute to specific roles essential for daily functioning. The cerebrum, the largest part of the brain, is responsible for higher cognitive functions such as reasoning, planning, and abstract thought. It is divided into two hemispheres, each containing four lobes: the frontal lobe, which is involved in voluntary movement, decision-making, problem-solving, and emotional regulation; the parietal lobe, which integrates sensory information and is crucial for spatial sense and navigation; the temporal lobe, which plays a significant role in processing auditory information, memory formation, and language comprehension; and the occipital lobe, which is primarily responsible for visual processing, interpreting visual stimuli such as light, color, and movement. Below

the cerebrum is the cerebellum, located at the base of the brain, which is essential for motor control, coordination, balance, and the learning of motor skills, helping to fine-tune voluntary movements to be smooth and accurate. The brainstem, composed of the midbrain, pons, and medulla oblongata, connects the cerebrum with the spinal cord and regulates vital autonomic functions such as heart rate, breathing, and sleep-wake cycles. Together, these regions coordinate a vast array of activities that underline human behavior, perception, and interaction with the environment (Azevedo et al., 2009).

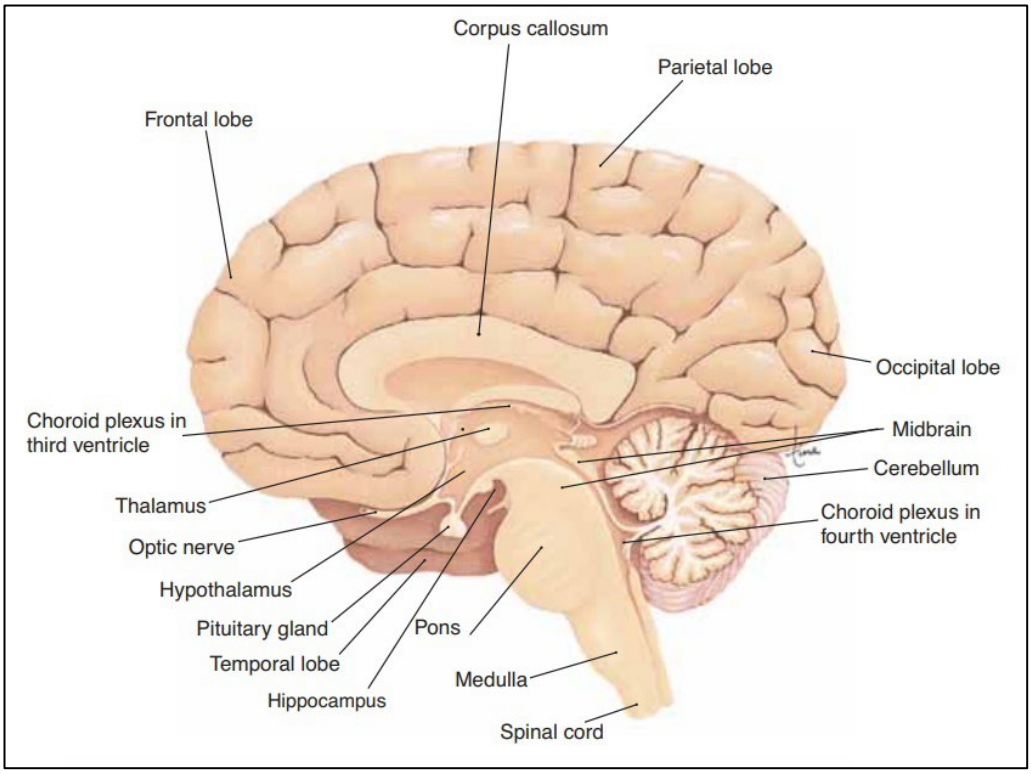

Figure 3.1 Brain structure (*The Brain - Anatomy and Physiology*, n.d.)

3.1.3.2. Measuring EEG

EEG records brain functioning in terms of electrical activity from neurons, especially the cortical ones. Such local circuits are involved in operations which use electrical impulses known as action potential and electrical fields arising

from the firing of numerous neurons in a local area. These fields are mainly produced by the post-synaptic activities at dendrites of the cortical pyramidal neurons which are oriented parallel to the surface of the cortex (Niedermeyer, E., Da Silva, F. L., et.al., 2004).

To record these electrical potentials ten electrodes are positioned on scalp based on the pattern which is known as 10-20 system or their variants like 10-10 or 10-5 system. Each electrode measures the fluctuations in voltage regarding a reference point and the variations in the voltage differences are measured. These signals are then amplified and then converted into digital format for analysis purposes.

3.1.3.3. 128-Channel EEG

128-Channel EEG is one of the most advanced electroencephalography systems in which 128 electrodes are strategically located at different locations of the scalp which in turn records the electrical activity of the brain. The placement of electrodes often conforms to the international 10–20 system and its derivatives affords a dense sampling of surface of cortex. Nevertheless, unlike the standard EEG systems with the reduced number of head electrodes, the 128-channel configuration provides a high in space density and both surface and source mapping of the brain activity since it is capable of collecting signals from different areas of the brain at the same time (Michel et al., 2004).

If one wants a more profound level of identification of the brain activity localization and dystheny details, one needs a 128-channel EEG. This is useful most especially in clinical and research scenarios. For example, in epilepsy monitoring, because of the higher resolution, one can identify epileptic foci, which are a necessity to carry out surgical operations. In cognitive neuroscience, the ability of a 128-channel EEG enables early identification of multiple types of cognition such as attention, memory and decision making from activity of neural locations that are relatively close to each other. Moreover, higher channel density in 128-channel EEG enhances the possibility of reconstructed cortical sources of electric signals in comparison with 10-20 electrode placement, which

helps in better understanding of functional brain connections and their changes in dynamics. This capability is very useful especially in applications, which involve the construction of brain computer interface or functional brain mapping and neurofeedback training, where the accurate localization and analysis of activity is critical to getting the best results (Cohen & Cuffin, 1983; Michel et al., 2004).

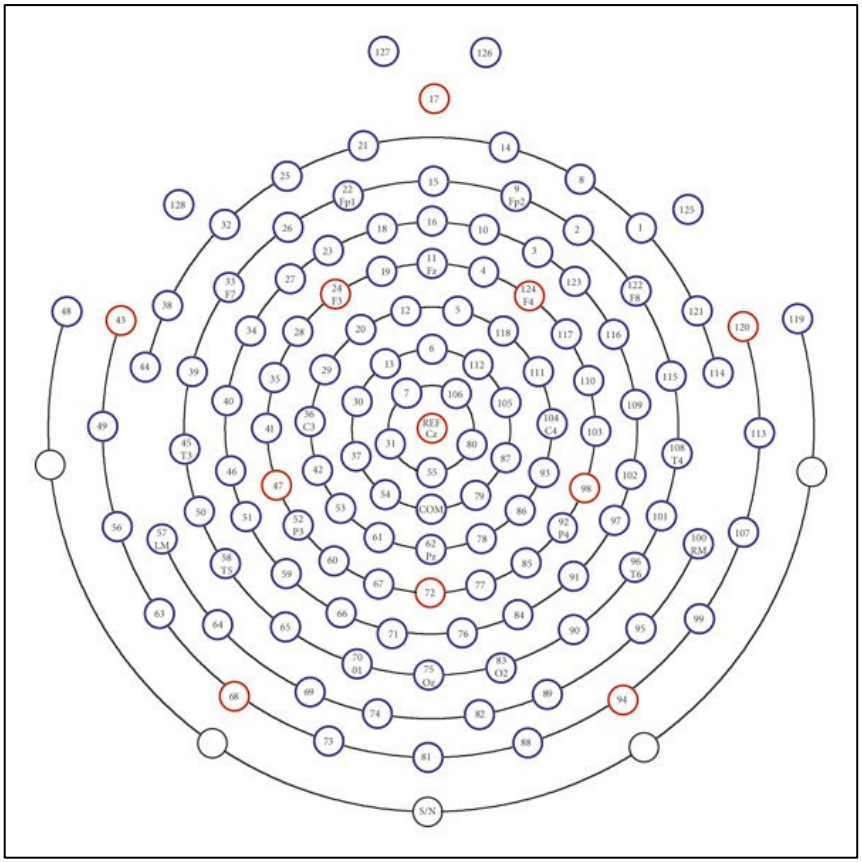

Figure 3.2 128-channel electrode placement (Chen et al., 2019)

The EEG system has a 10-10 or 10-20 electrode positioning system which each channel corresponds to specific brain analysis.

Frontal Lobe

- FP1, FP2: These channels represent the prefrontal region of the brain because this part of the brain is located at the frontal lobes and contributes to the functions such as decision making, planning and personality (Koessler et al., 2009).
- F3, F4, F7, F8: These electrodes are located over the frontopolar and presupplementary motor areas and play a key role in problem-solving and other coefficients of higher cortical tone (Caspers et al., 2011).
- AF3, AF4: Relating to the higher cognitive activities in front-most part of the frontal lobe involving planning and personality (Michel & Brunet, 2019).

Central Area (Motor Cortex)

- C3, C4, Cz: These channels are in accordance with the primary motor cortex. C3 is situated over the left motor cortex that controls voluntary movements on the right half of the body while C4 is situated over the right motor cortex, which initiates voluntary movements on the left half of the body (Koessler et al., 2009).
- CP1, CP2: Located above the Cheyne stokes reserve and near the central sulcus, these channels deal with somatosensory cortex that allows recognition of sensations from distinct areas of the body (Michel & Brunet, 2019).

Parietal Lobe

- P3, P4, Pz: These electrodes can be said to locate with the parietal cortex which has the function of integration of sensory information and participation in spatial orientation and movement (Caspers et al., 2011).
- P7, P8: Situated in the parietal region, these channels play a role incorporating the analysis of the sensory inputs and perform spatial cognition (Koessler et al., 2009).

Temporal Lobe

- T7, T8: These montages are placed over the temporal regions and temporal loops which are associated with language, auditory as well as memory essentials(Brodbeck et al., 2018).
- Positive electrodes: FT7, FT8: These electrodes are located at the frontal temporal region that assists in processing sound and language personality (Michel & Brunet, 2019).
- TP7, TP8: Located over the posterior temporal regions, these are the areas related to memory handling and sensory integration (Koessler et al., 2009).

Occipital Lobe

- O1, O2: These channels are located over the occipital lobe – the primary cortex concerned with vision (Brodbeck et al., 2018).
- PO3, PO4: As both channels are found in the parieto-occipital area, these channels help in processing sensory inputs together with visual information (Caspers et al., 2011).

Midline Electrodes

- Fz: Positioned in the superior frontal gyrus and part of the limbic system hence, it sub serves attention and executive control (Luck, 2014).
- Cz: Situated at the vertex of the head, Cz is dual representing the motor and the sensory cortex in the midline personality (Michel & Brunet, 2019).
- Pz: This channel is located over midline parietal cortex and help in sensory integration of space or space awareness (Caspers et al., 2011).
- Oz: Oz electrode position is on the midline of occipital lobe and its major functions are related to vision (Brodbeck et al., 2018).

Additional Specific Channels

- F1, F2, FC1, FC2: These channels are located in the intermediate regions between the frontalis, central, and parietal electrodes and they are involved in motor coordination and sensory functions personality (Michel & Brunet, 2019).
- Iz: Comes close to the inion region near the occipital midline and is frequently employed in visual investigations (Luck, 2014).

According to the channel specification, in our study, we will use FP1 and FP2 electrodes to examine decision-making process, F7 and F8 electrodes to examine cognitive behavior and O1 and O2 electrodes to examine eye movements effect.

Tablo 3.1 Corresponding channel number to the electrode (*128Ch Standard-BrainCap for TMS with Multitrodes Electrode Layout and Channel Assignment*, n.d.)

Channel Number	Name	Channel Number	Name
1	Fp1	65	FFC1h
2	Fp2	66	FFC2h
3	F3	67	CCP1h
4	F4	68	CCP2h
5	C3	69	AFF1h
6	C4	70	AFF2h
7	P3	71	PPO1h
8	P4	72	PPO2h
9	O1	73	FCC3h
10	O2	74	FCC4h
11	F7	75	CPP3h
12	F8	76	CPP4h
13	T7	77	FFC5h
14	T8	78	FFC6h
15	P7	79	CCP5h
16	P8	80	CCP6h
17	Fz	81	FTT7h

Tablo 3.1 cont. Corresponding channel number to the electrode (*128Ch Standard-BrainCap for TMS with Multitrodes Electrode Layout and Channel Assignment*, n.d.)

18	Cz	82	FTT8h
19	Pz	83	TPP7h
20	IO	84	TPP8h
21	FC1	85	PPO9h
22	FC2	86	PPO10h
23	CP1	87	OI1h
24	CP2	88	OI2h
25	FC5	89	F9
26	FC6	90	F10
27	CP5	91	P9
28	CP6	92	P10
29	FT9	93	PO9
30	FT10	94	PO10
31	TP9	95	O9
32	TP10	96	O10
33	F1	97	FCC1h
34	F2	98	FCC2h
35	C1	99	CPP1h
36	C2	100	CPP2h
37	P1	101	FFC3h
38	P2	102	FFC4h
39	AF3	103	CCP3h
40	AF4	104	CCP4h
41	FC3	105	AFp1
42	FC4	106	AFp2
43	CP3	null	null
44	CP4	107	POO1
45	PO3	108	POO2
46	PO4	109	AFF5h
47	F5	110	AFF6h
48	F6	111	FCC5h
49	C5	112	FCC6h
50	C6	113	CPP5h
51	P5	114	CPP6h

Tablo 3.1 cont. Corresponding channel number to the electrode (*128Ch Standard-BrainCap for TMS with Multitrodes Electrode Layout and Channel Assignment*, n.d.)

52	P6	115	PPO5h
53	AF7	116	PPO6h
54	AF8	117	FFT7h
55	FT7	118	FFT8h
56	FT8	119	TTP7h
57	TP7	120	TTP8h
58	TP8	121	FFT9h
59	PO7	122	FFT10h
60	PO8	123	TPP9h
61	Fpz	124	TPP10h
62	CPz	125	POO9h
63	POz	126	POO10h
64	Oz	127	Iz
		Gnd	Afz
		Ref	FCz

3.1.3.4. EEG Frequency Bands

EEG signals are composed of multiple frequency bands, each associated with different physiological states and cognitive functions: These EEG signals are a combination of different frequency bands where each band relates to specific physiological state and or cognitive activity.

Delta Waves (0. 5 - 4 Hz): These are the slowest rhythms, and they have a high amplitude of oscillations. They are mainly apparent during NREM sleep which is in the process of firm sleep, preferably in children under the age of five years. Delta waves are also involved in restorative processes during sleep and features are identified in various diseases, as trauma or brain infarctions (Bronzino, 2000).

Theta Waves (4 - 8 Hz): It is recorded commonly in daydreaming, lightly sleeping, very light meditating and problem solving in imaginative ways. In the adult brain theta activity is associated with memory function as well as selective

memory retrieval and affective processing/ In children the same sort of theta activity is observed during high cognitive operations (Bronzino, 2000).

Alpha Waves (8 - 13 Hz): Alpha activity is found to occur mainly from the posterior regions of the brain; especially the occipital region during the awake states, especially when the eyes are closed. Alpha waves are associated with a state of wakeful rest and have been said to have middle sensory attached signal inputs to cortical processors of the brain (Bronzino, 2000).

Beta Waves (13 - 30 Hz): These are fast waves, and they have a low voltage, and they are associated with wakefulness, alertness, or anxiety. Beta wave activity is experienced during attempts to focus, to think analytically or to perform other forms of higher mental activities. Beta activity reveals activity of the brain which can be abnormally elevated; this has been linked to anxiety and other illnesses (Bronzino, 2000).

Gamma Waves (30 - 100 Hz and above): Gamma waves have their frequency above 30 Hz and these are related to the upper part of the brain as well as the high-end cognitive functions such as perception, attention, learning and especially the encoding of information to be stored in the brain. Gamma oscillations, therefore, might be related to the co-ordinate firing of neurons in functionally distinct parts of the cortex and may offer the means for combining and uniting various form and contents of conscious experience (Bronzino, 2000).

3.1.4. Gamma Oscillation

The brainwave that is associated with cognitive function including attention, memory and conscious perception is brainwave called gamma oscillations. Gamma oscillations is one of the fastest brainwave frequencies which fall within the 30 to 100 Hz range (Jensen & Mazaheri, 2010).

The reason to study gamma oscillation in cognitive neuroscience is the belief on their involvement in higher-order cognitive processes, like decision-making, problem-solving and the integration of information across different areas of the brain (Uhlhaas & Singer, 2010). The various neurological disorders

like schizophrenia and Alzheimer's disease are linked to abnormal gamma activities (Smith & Doe, 2024).

During tasks involving visual processing or sustained attention, there might be physiological interaction between the systems generating EOG signals and those generating gamma band oscillations, such as when focusing on a visual target. The coordination between eye movements and cortical gamma activity could reflect a coupling between sensory processing and motor control, facilitating efficient perception and action. Moreover, both EOG and gamma band EEG signals might share common underlying neural mechanisms, particularly in tasks requiring visuomotor integration, as regions involved in controlling eye movements, such as the frontal eye fields, interact with cortical areas generating gamma oscillations. This indicates that gamma band activity may play a role in the timing and coordination of eye movements, linking the physiological processes captured by EOG with those reflected in gamma band EEG. In summary, EOG signals and gamma band EEG oscillations, while originating from different physiological sources, are functionally related in tasks involving visual processing, attention, and eye movement control, reflecting the complex integration of sensory, cognitive, and motor processes in the brain.

3.1.5. Electrooculogram

Electrooculography is used to study the movements of the eyeball. EOG is a measure of the electrical potential in pigment epithelium layer in retina. Electrooculography uses the electrical potential difference created by polarization between the cornea and eye retina. This potential which is created in retina pigment epithelium layer changes by eyeball movements. The observation shows that the cornea is electrically positive when compared to the back of the eye. The movement of the eye recorded by electrooculography (Reilly & Lee, 2010).

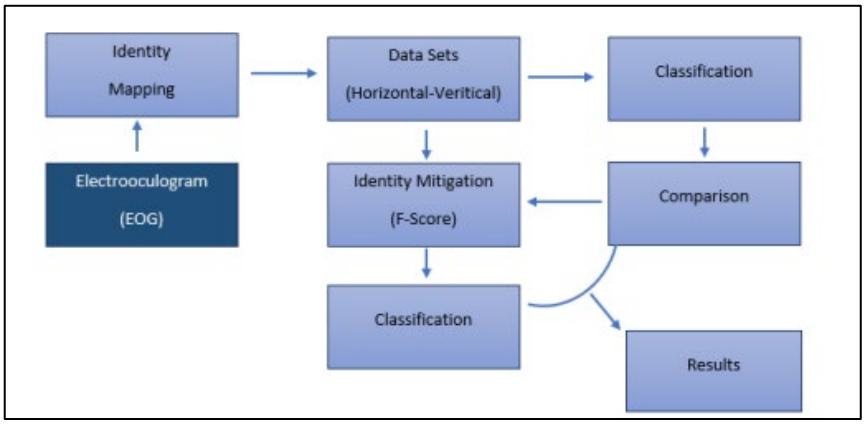

Figure 3.3 Electrooculogram Processing (Reilly & Lee, 2010)

3.1.5.1. Eye Anatomy

Approximately 80% of human perception occurs in the eye which is the five basic sensory organs of humans. The eye is placed in a bone socket called orbita in the skull and covered with soft fatty tissue. The movement of the eye is controlled by six muscles. The optic nerves connect the eye with the brain. The sclera, which is white and fibrous in the outermost part, bends in front, becomes transparent and takes the name of cornea. There are no photosensitive receptors on the optic disc, which is the exit point of the optic nerves. There is a pigmented vein layer (choroid) between the retina and the sclera, which forms the forward extension of the ciliary body and iris. The light coming into the eye passes first to the cornea layer, the two surfaces of which are parallel. After the cornea, the rays transit the pupilla in iris reach the crystal lens. The beam passing through the glassy body dropped onto the fovea on the vascular layer. The image falling on the fovea is upside down. In the brain, the image is corrected and detected (Moini, 2019).

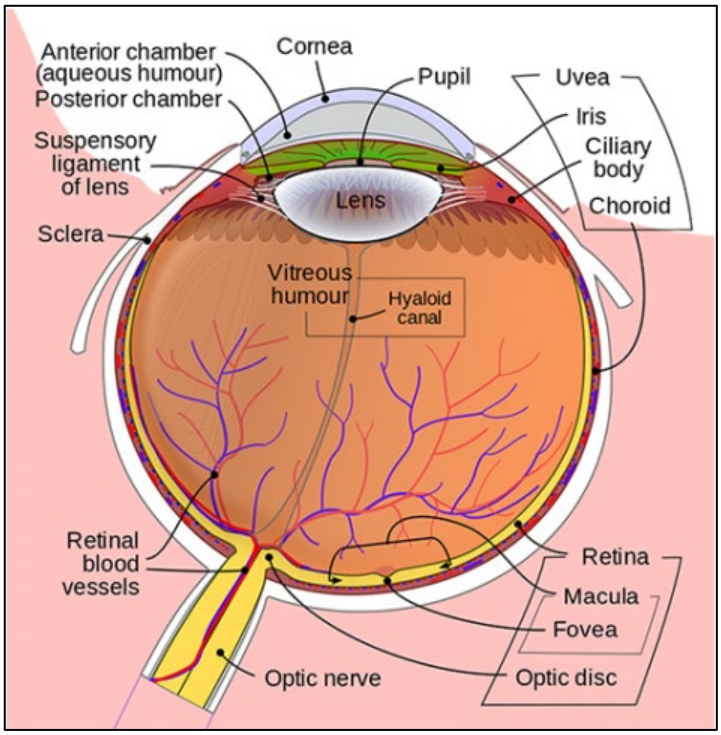

Figure 3.4 Physiology of Eyes (Moini, 2019)

3.1.5.2. Eye Muscle

The eye moves on two axes, vertical and torsional axis. These axes and the eyeball meet at the middle point. Eye movements are provided by simultaneous contraction and relaxation of six eye muscles. Eye muscles are different in structure from other skeletal muscles. The nerve connections of the muscles are very dense. The eye muscles have high activity and contain a lot of mitochondria. Eye muscles are among the fastest contracting muscles in the human body (Moini, 2019).

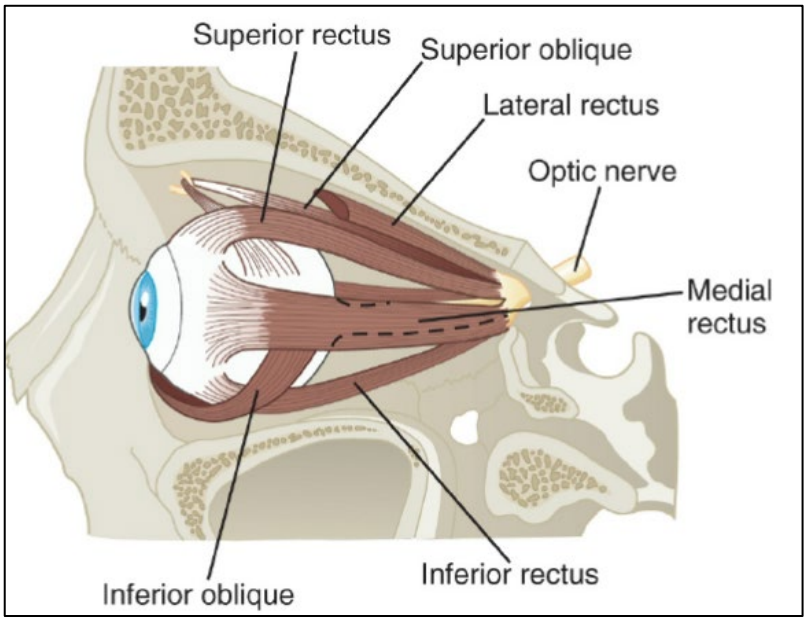

Figure 3.5 Eye Muscle (Moini, 2019)

3.1.5.3. Measurement And Analyzing of EOG Signals

Eye movements can be detected by placing electrodes on the skin in the head around the eyes.

A pair of electrodes are placed either above and below or right and left of the eye. When the eye moves from center to one of the electrodes, it measure the positive side of the retina and then others measure the negative side. The potential difference occurs between these two electrodes (Heo et al., 2017).

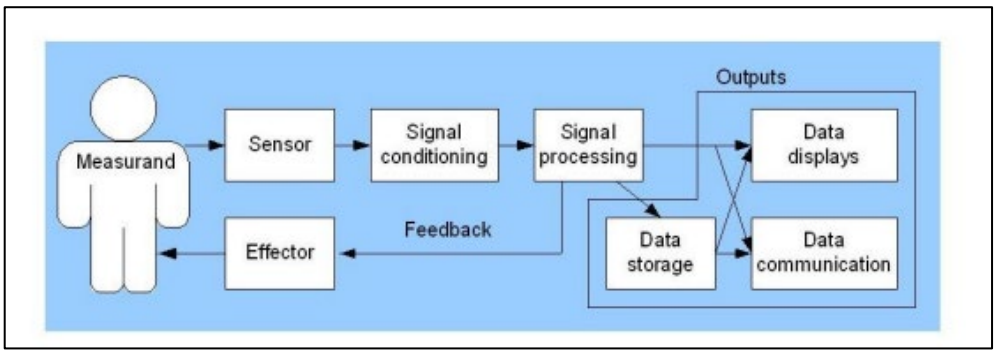

Figure 3.6 EOG Measurement (Heo et al., 2017)

3.1.5.4. Factors That Affect EOG Measurement

EOG signals can be affected by many factors. These; placement of electrodes, pre-adaption time, pupil dilatation, exophthalmos, cone fundal potential, contact surface connection of electrodes, speed of eye movements, age, sex, and light intensity in the environment (Reilly & Lee, 2010).

3.1.5.5. Phase Space Analysis

Phase space analysis is a valuable strategy employed to investigate the popular EOG signals —the electrical potential difference records obtained by electrodes positioned around the eyes that analyze and record eye movements. This method is very sensitive for identifying and interpreting various patterns and behaviors in EOG data especially in relation to cognitive abilities or neurological disorders or when observing visual tracking tasks (Iasemidis et al., 2003).

In the phase space of analysis, the EOG signal is described as a time series in n-dimensional phase space where each dimension is the signal, or a derivative of the signal such as velocity or acceleration. In this way, the transformation enables researchers to monitor the system’s behavior in the course of time and to identify changes which could hardly be seen if the time-domain signal had been analyzed. For instance, rhythmic or oscillatory behaviors may be seen as cyclic structures such as saccades (rapid eye movements of the eyes) or fixations, or even as identifiable loops or formations in phase space (Babloyantz, 1987).

3.1.6. Cognitive Decision

The mental process of choosing between different options or actions based on thought, reasoning, and judgment are referred to as a cognitive decision. Cognitive functions such as perception, memory, attention, and problem solving participate in the cognitive decision-making process. During the cognitive decision-making process, individuals considered each option's pros and cons, potential outcomes then decided based on this evaluation (Simon, 1955).

Experience, knowledge, emotions, and external stimuli are the same factors that affect cognitive decision-making (Shafir & LeBoeuf, 2002). This has a crucial effect on everyday life like it allows individuals to achieve goals, solve complex situations, and solve problems (Gold & Shadlen, 2007). The cognitive decision-making will be investigated in the study through the brain activity (via Electroencephalogram (EEG) gamma oscillations) and eye-tracking data (via Electrooculogram (EOG)), which will be provide explanation into how decisions are made, and the neural mechanisms underline these processes.

3.1.7. Cross Power Spectral Density (CPSD)

The relationship between two signals in the frequency domain is measured by cross power spectral density (CPSD). It gives information about how correlated the two signals are as a function of frequency and explains the power distribution of two signal over frequency. The concept of CPSD can be quite helpful in telecommunications, control systems, vibration or operational modal analysis, and biomedical engineering, to name a few areas, where signal interaction is of interest (Oppenheim & Schafer, 2009; Yanwei Wang et al., 2005).

The Cross Power Spectral Density, $S_{xy}(f)$, of two signals $x(t)$ and $y(t)$ describes the sharing of power crossed with one another at frequency $f = \omega/2\pi$, with f being the frequency in the case of the CPSD. The CPSD conveys how much of the total power content of the signals x and y, shows as shared content through correlation at frequency f. It will also show the amount of noise in either signal, as viewed through the lens of cross-correlation (Oppenheim & Schafer, 2009).

Mathematically, the CPSD is defined as the Fourier transform of the cross-correlation function $R_{xy}(\tau)$, between signals $x(t)$ and $y(t)$:

$$\boldsymbol{S_{xy}(f) = \int_{-\infty}^{\infty} R_{xy}(\tau) e^{-j2\pi g\tau} d\tau} \qquad (3\text{-}6)$$

where:

Cross Power Spectral Density function is $S_{xy}(f)$

The cross-correlation function of $x(t)$ and $y(t)$is $R_{xy}(\tau)$

Frequency variable is f

Time lag variable is τ

Imaginary unit is j (Yanwei Wang et al., 2005)

CPSD can be used in coherence analysis. The coherence function between two signals, which measures the degree of linear correlation between the signals at various frequencies, is computed using the CPSD.

$$\boldsymbol{C_{xy}(f) = \frac{|S_{xy}(f)|^2}{S_{xx}(f)S_{yy}(f)}} \quad (3\text{-}7)$$

where:

Coherence function is $C_{xy}(f)$

Power spectral density is $S_{xx}(f)$ and $S_{yy}(f)$ of $x(t)$ and $y(t)$, respectively (Yanwei Wang et al., 2005).

The CPSD used in biomedical signal processing such as in neuroscience to analyze brain signals, connectivity determination or different brain region synchronization (Blinowska, 2011).

3.1.8. Hilbert Transform and Phase-to-Amplitude Coupling

Given a single-channel EEG signal $x(t) \in R^N$, where N is the number of time samples is, the Hilbert transform ($\mathcal{H}\{x(t)\}$) is used to create the corresponding analytic signal $\mathcal{H}(t)$ as follows:

$$\boldsymbol{\hat{x}(t) = \mathcal{H}\{x(t)\} = \frac{1}{\pi} P.V. \int_{-\infty}^{\infty} \frac{x(\tau)}{t-\tau}\, d\tau} \quad (3\text{-}8)$$

where P.V. denotes the Cauchy principal value of the integral. The Hilbert transform produces an analytic signal $z(t)$, which is a complex representation of original signals:

$$\boldsymbol{z(t) = x(t) + j\hat{x}(t) = A(t)e^{j\phi(t)}} \quad (3\text{-}9)$$

where $A(t)$ and $\phi(t)$ represent the instantaneous amplitude and instantaneous phase of the signal, respectively, which are defined as follows for single channel:

$$\boldsymbol{A(t) = \sqrt{x^2(t) + \mathcal{H}\{x(t)\}^2}} \tag{3-10}$$

$$\boldsymbol{\phi(t) = \arctan \frac{\mathcal{H}\{x(t)\}}{x(t)}} \tag{3-11}$$

where $-\pi < \phi < \pi$

Phase amplitude coupling measures the degree to which the high frequency power is modulated by the phase of the EOG, low-frequency oscillations.

To quantify PAC, Magnitude Squared Coherence Analysis is used. The raw EEG signals were filtered in the high-frequency Gamma band (30–100 Hz) and low-frequency EOG (1–12 Hz) oscillations (Adriano et al., 2010).

3.1.9. Magnitude Squared Coherence Analysis of multichannel analytic square of amplitude and phase signals

For our multi-EEG/multi-EOG channel approach, the multiple-coherence function becomes

$$\boldsymbol{C_{X\phi_i}(f) = \frac{P^{\dagger}_{X_{\phi_i}}(f) P^{-1}_{XX}(f) P_{X_{\phi_i}}(f)}{P_{\phi_i\phi_i}(f)}} \tag{3-12}$$

for the i th channel signal which are related to EOG parameters,

$P_{X_{\phi_i}}(f) = A^2_{Fp1} * \phi_i$ for each EEG channel.

where:

- X vector corresponds to the array of $m = 4$ channels (FP1,FP2,F7,F8) where $\{A^2_{Fp1} * \phi_i, A^2_{Fp2} * \phi_i, A^2_{F7} * \phi_i, A^2_{F8} * \phi_i\}$ represent the instantaneous power and phase coupling for each EOG channel index, i
- $P_{X\phi_i}$ is the 3-dimensional vector of cross power spectral densities between the EEG channels and one of the EOG channels, $\emptyset_i$ (VEOG,HEOG, PS).

- P_{XX} is the m-by- m matrix of power spectral densities and cross power spectral densities of the EEG channels.
- $P_{\phi_i\phi_i}$ is the power spectral density of each EOG channel (VEOG,HEOG, Pupil Size).
- (†) stands for the complex conjugate transpose.,

We obtained Magnitude Squared Coherence Analysis of 12 channel analytic square of amplitude and phase signals denoting partial synchronizations over spatial domain between cognitive gamma band and EOG parameters like pupil size. We implement $C_{X\phi_i}(f)$ as phase-amplitude-coupling of each channel for a given f frequency (MI).

3.2. METHODOLOGY

3.2.1. Dataset Method

Open data-based is used in this thesis which is EEGEyeNet dataset. The dataset has two sets of preprocessed data minimally and maximally preprocessed with the raw data. By doing this, they minimize the experimental barrier by offering ready-to-use clean data, enabling users to work with raw data (Smith & Doe, 2024).

3.2.1.1. Data acquisition

Participants: 356 healthy adults participated in the study. The ages between 18 and 80 years which 190 female and 166 male participants.

Recording setup: By using a 128-channel EEG system, high-density EEG data was recorded at 500 Hz sampling rate. Before every recording session, the impedance of every electrode was measured and maintained below 40kOhm. Eye position was simultaneously collected at 500 Hz sampling rate and less than 0.01° root mean square (RMS) of the distances between subsequent samples using an infrared video-based ET EyeLink 1000 Plus from SR Research. Before every recording, the ET was calibrated using a 9-point grid. The ET calibration

was repeated in a validation phase until the average error for all points was less than one, or the error between two measurements at any location was less than 0.5°. The participants were positioned 68 centimeters away from a 24-inch display featuring an 800x600 pixel resolution. A chin rest was used to ensure a steady head position (Smith & Doe, 2024).

3.2.1.2. Preprocessing

Filtering is an important step to guarantee the quality of the EEG data, mainly because this signal is quite often contaminated by artifacts. For the pre-processing of the EEGEyeNet dataset reference tools by Pedroni et al. was used with options representative of both minimal as well as maximal pre-processing techniques. Special preprocessing included identification and estimation of bad electrodes plus applying 40 Hz high-pass filter and 0. 5 Hz low-pass filter. Conversely, maximal preprocessing entailed the erasure of multiple artefacts in the fMRI signal like muscle, heart, and ocular noise through Independent Component Analysis accompanied by a pre-specified classifier known as ICLabel. This preprocessing allows for the final dataset which is free of many artifacts that characterize raw EEG data for neuroscientific use (Smith & Doe, 2024).

3.2.1.3. Data Annotation

Eye movements were annotated into three distinct events: Saccades which are quick movements of the eyes, fixations which involves the fixation of the eyes at any object and blinks which are involuntary shutters of the eyes. A saccade is a rapid change of gaze direction from one object to another, fixation is not at any time on a saccade, and blinks are taken as a special type of fixation for which the area of the pupil is zero. For each of the experimental paradigms, annotations specify the onset and offset of such events, as well as positions (Smith & Doe, 2024).

3.2.1.4. Experimental Paradigms

The data include the Experiment paradigm one which comprises data recorded when performing simple prompting tasks, the second Experiment paradigm one which contains data gathered when performing delayed prompting tasks and the third Experiment paradigm one which contains data gathered when performing delayed object recognition tasks. These paradigms offer a set of data that is particularly valuable for investigation of the relation between the EEG signals and eye movements (Smith & Doe, 2024).

The pro- and anti-saccade used in this study conforms with the international standard for ant saccade procedure. Every trial starts with the appearance of a fixation square in the middle of the screen, to which the participants are told to direct their attention for the time, selected randomly from the range of 1 to 3. 5 seconds. After this, a cue is displayed either on the left or right side of the central fixation square (Smith & Doe, 2024).

3.2.1.5. Prosaccade Trials

In the prosaccade trials the subject is told to look at the cue the moment it is introduced to the visual field. The cue is visible for one second; then the participants are forced to re-attend to the center of the screen.

This paradigm is useful to several types of research, for example, to estimate the direction of gaze and with the participant's reaction to inhibition, both of which are valuable orientations to cognitive and neurological functions (Smith & Doe, 2024).

3.2.1.6. Gaze Direction Determination Task

The task in the benchmark is to establish to which side of the subject the face is rotated along a horizontal plane. This task is solely derived from the first experimental paradigm, that is, the Pro- and Ant saccade paradigm. For all samples used in this task it was ensured that the participant made a saccade towards the correct direction and then fixated on the cue. Such was the case if a

participant did not follow this sequence the respective sample was eliminated from the samples collection (Smith & Doe, 2024).

Since the anti-saccade task is a type of measure of behavioral inhibition abilities and the concern is in saccade direction, the ant saccade task was simplified by only using data from the prosaccade trials of the ant saccade task. In this task, 30,842 samples have been employed, and 14,827 of them belong to the “left” label, and 16,015 belong to the “right” label (Smith & Doe, 2024).

The beginning of each sample occurs when the cue is presented on the screen and each sample contains on average one saccade. The saccade information to be encoded must be categorized between a left or right saccade, hence the classification is binary. The measure of performance for this task is accuracy, a baseline for which is randomly generated text of 52. 3% that is obtained from the majority class. Even though this task seems basic, the correct estimation of horizontal direction of human gaze is highly significant for numerous practical purposes (Smith & Doe, 2024).

3.2.2. Analyzing of Signal

3.2.2.1. Data Acquisition

The study used the data which were collected from simultaneous EEG and eye tracking recordings of the dataset. The data involved the EEG signals’ channel and eye movement measures, such as horizontal movements, vertical movements, and pupil diameter. The EEG data was sampled at a frequency of 500 Hz.

3.2.2.2. Signal Preprocessing

Concerning the preprocessing of the recorded signals, several steps were followed in the process. To begin with, the EEG data from the loaded dataset was obtained and cast to double for the sake of numerical precision in the subsequent processing. Also, for analyzing EEG data we extracted the horizontal, vertical, and pupil size eye movement signals (EOG signals). For the

elimination of high-frequency noise, the EOG samples were filtered with 30th order Butterworth low-pass filter with cutoff frequency of 50 Hz. This filtering was done through zero-phase filtering (`*filtfilt*' function) to prevent phase distortion. Furthermore, only the high pass filtered EOG signal was used since the cutoff frequency was set with 12 Hz to filter out low-frequency content. The signals obtained were then normalized between -1 and 1 to make the comparisons easier and the subsequent analysis.

For coherence analysis in this study, the EEG and EOG signals were organized into two matrices that are explained next. The raw data were gathered from six electrode sites, FP1, FP2, F7, F8, O1 and O2, and arranged in a matrix form as "*X_matrix*" after detrending to minimize the coherence artefact. In "*X_matrix*" each row corresponds to specific electrode which are FP1 and FP2 at the left and right frontal poles, F7 and F8 at frontal site from left side and right side respectively O1 and O2 from left occipital side and right occipital side, respectively. Likewise, the EOG data were structured in terms of a matrix referred to as "*Y_Matrix*" which holds the filtered signals for horizontal eye movement, vertical eye movement, and the variations in the size of the pupil. These matrices enabled a systematic comparison of phase amplitude coupling of the EEG and EOG signals acquired during different brain regions and eye movement types.

3.2.2.3. Phase Space Analysis

The analysis done here used phase space to try to understand how the different signals that make up the EOG move in relation to each other. The phase space plot analysis was conducted to determine connection between the horizontal and vertical eye movements. Another plot was developed to attend to the effects of horizontal eye movements and pupils. Finally, a phase space plot was created in order to observe the relationship between the subject's vertical fluctuations and pupil dilations.

3.2.2.4. Frequency Filtering and Band Analysis

After having performed frequency filtering, the steps that are followed are band analysis.

Frequency bands of the EEG data were classified using frequency range limits that are standard in neuroscience. The bands incorporated included the Delta band (0.5 – 4 Hz), Theta band (4- 8 Hz), Alpha band (8- 13 Hz), Beta band (13-30 Hz) and the Gamma band (30-100 Hz). For each frequency band, a 100th-order FIR bandpass filter was designed and used to extract required brain wave components. By using '*filtfilt*' the phase shift does not affect the signals since they are bandpass filtered at this stage.

3.2.2.5. Cross Power Spectral Density (CPSD) Analysis

The latter is more specifically defined as the Cross Power Spectral Density (CPSD) analysis.

Since, the power spectral relationship between the various EOG signals needed to be assessed, CPSD analysis was called for. The high pass filtered signals were further processed to calculate the CPSD between horizontal and vertical eye movements as well as the intersample CPSD between the pupil size signal. For spectral analysis, a window of 256 samples with 50% overlap was employed, mean, and the number of points of the Fast Fourier Transform (FFT) was 512.

3.2.2.6. EEG Analysis

Regarding gamma oscillations, information from the EEG recording was also subjected to analysis with the purpose of establishing involvement of the gamma frequency band. The filtered signals of gamma frequency (30–100 Hz) were extracted only for the selected channels FP1, FP2, F7, F8, O1 and O2. The signals acquired were filtered and the gamma activity was obtained after detrending the signals with the help of a reference channel.

3.2.2.7. Coherence Analysis

To quantify the similarity between the EEG signals and the EOG signals, animals underwent a quantitative analysis with the help of magnitude-squared coherence algorithm. A Hamming window of 256 samples with 50 percent overlap was applied while calculating the coherence between the EEG signals and the EOG signals. Coherence was studied for several pair of EEG and EOG channels to determine the relationship between brain oscillations and eye movements.

3.2.2.8. Hilbert Transform and Phase-to-Amplitude Coupling Analysis

Using Hilbert Transform we investigate how a phase relates to an amplitude of some EEG signals. The measurement of instantaneous phase and amplitude of a signal is a mathematical technique that is widely used in neuroscience known as the Hilbert Transform. We apply this transform and the same can also be used to decompose EEG signals into their phase and amplitude components for the study of phase to amplitude coupling (PAC). It is important to analyze PAC to achieve an understanding in dynamic interactions of different frequency bands from EEG signals. It specifically measures the amount by which the amplitude of a high frequency oscillation varies when the phase of a low frequency oscillation is modified. Here we analyze a study of the coupling between theta (4–7 Hz) phase and gamma (30–100 Hz) amplitude and its relationship to cognitive processes including decision making and attention. To implement the PAC analysis, we first ran bandpass filtering on the raw EEG data to isolate the theta and gamma frequency bands. The instantaneous phase of the theta band and the instantaneous amplitude of the gamma band were extracted then using the Hilbert Transform. To quantify the coupling strength between these oscillations, we computed the modulation index (MI). This let us look at how neural activity is synchronized across different brain regions to inform us of the functional connectivity related to cognitive decision-making tasks. The analysis also indicated strong phase amplitude coupling, particularly between

channels F7, FP1, both indicating a role for frontal brain activity in eye movement artefacts and cognitive function.

3.2.2.9. Statistical Analysis

To get further confirmation, coherence values are represented in figures to describe the PAC between different channels. Histograms were used to study the probability distribution of coherence values to appreciate the statistical properties of the signal coupling.

To reveal the influence of eye movements on gamma oscillation patterns in the frontal and, particularly, occipital brain areas, both phase and amplitude of EEG signals were compared to EOG data using surface plots. These multidimensional data relationships were well described by the "*surf"* command in MATLAB, thus allowing identification of specific frequency bands where artifact contamination is most prominent.

CHAPTER 4

4. EXPERIMENTAL FINDINGS AND ANALYSIS

This section will summarize the findings of the study. The analysis of EEG and EOG data were made by using MATLAB program. The data were taken from an open-source database called EEGEyeNet. The large grid paradigm task data are used in this study to examine the EEG-gamma oscillations and eye tracking (EOG) data during cognitive decision-making process.

Firstly, we load the data into the system and then transfer the data into double and store the sample frequency taken from the data as fs. The analysis start with EOG data. The corresponding eye tracking signals are on channel 131 for horizontal movement, 132 for vertical movement and 133 for pupil size. The relationship between time and the raw eye-tracking and pupil size data were visualized.

We designed a finite impulse response filter (FIR) to remove noise and irrelevant low-frequency components from the signals. The cut-off frequency is determined as 50Hz, and order is 30. The signals are also rescaled between -1 to 1 before visualizing.

The comparison between raw and filtered EOG was made by plotting. The graphs below show a comparison of horizontal movement, vertical movement, and pupil size of the eye, respectively.

The general findings for unfiltered data were that it shows broad range of eye movement from 0 to 1500 units, signals is noisy with rapid movements or artifacts. The sudden changes which are also called high-frequency components are seen in the data caused by noise or involuntary eyeblinks.

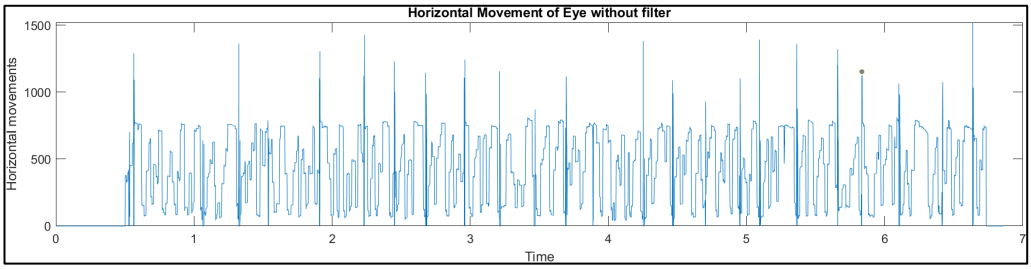

Figure 4.1 Horizontal Movement of Eye without Filter

The filtered signal characteristics shows that with noise reduction it seems smoother, and data shows a narrower range with the constrained values between -1 and 1. With the attenuation of high-frequency component, signal becomes clearer, and movement of eye pattern is apparent.

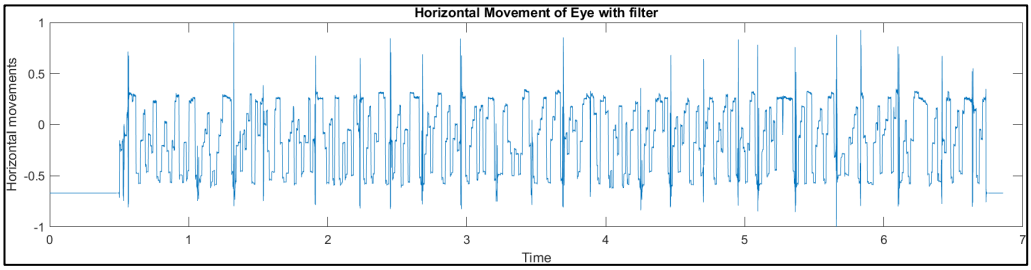

Figure 4.2 Horizontal Movement of Eye with Filter

The comparison of Figure 4-1 and Figure 4-2 will show us with the filtered signal eye movement data cleared from noise by reduction and outer artifacts. This filtering allowed us to make more precise analysis of the eye movement patterns.

When comparing the graphs (Figure 4-3 and Figure 4-4), we are examining the filtering effect on eye movement data. The first graph (Figure 4-3), with a vertical axis of approximately 0 to 600, represents a raw signal with considerable noise as evinced by sharp peaks and dips. In contrast, the second graph (Figure 4-4) presents the vertical axis with a sharp range from -1 to 1, indicating the signal has been normalized or has had noise associated with filtering. The filtered version of the graph appears smoother and more stable, with significantly

reduced noise, supporting the sparse signal structure in eye movement. In both graphs, we can observe similar trends of eye movement over time but what distinguishes them is the second graph presents a clearer view of the data in a filtered version of the signal while maintaining the signal structure and removing the noise. The secondary observation highlights that filtering of any mode of data can enhance signals for quality to be applied in the analysis of pertinent studies. This type of enhancement is, and should be, valuable in terms of reducing variability in quality of eye movement data in neurophysiology and on a more general stroke of semantic studies and precision.

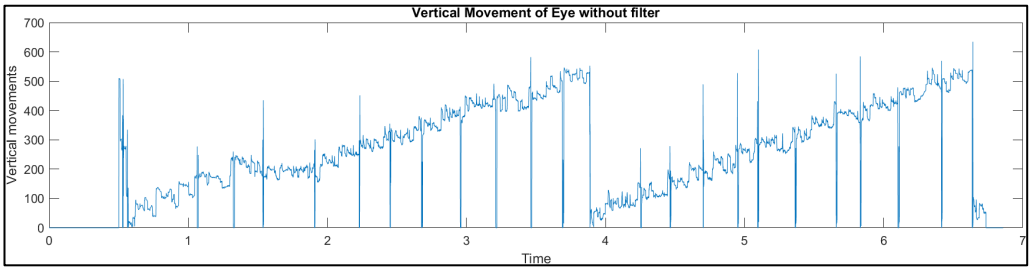

Figure 4.3 Vertical Movement of Eye without Filter

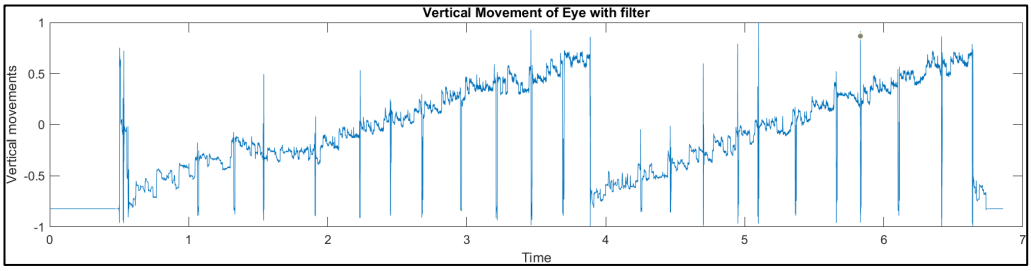

Figure 4.4 Vertical Movement of Eye with Filter

The comparison of pupil size over time with and without filters was made. The first graph (Figure 4-5) shows data from 0 to 1500 which indicates the noise presence with sharp spikes. The second graph (Figure 4-6) significantly normalized and reduced the noise. The filters improves the data quality and make the signal suitable for accurate analysis.

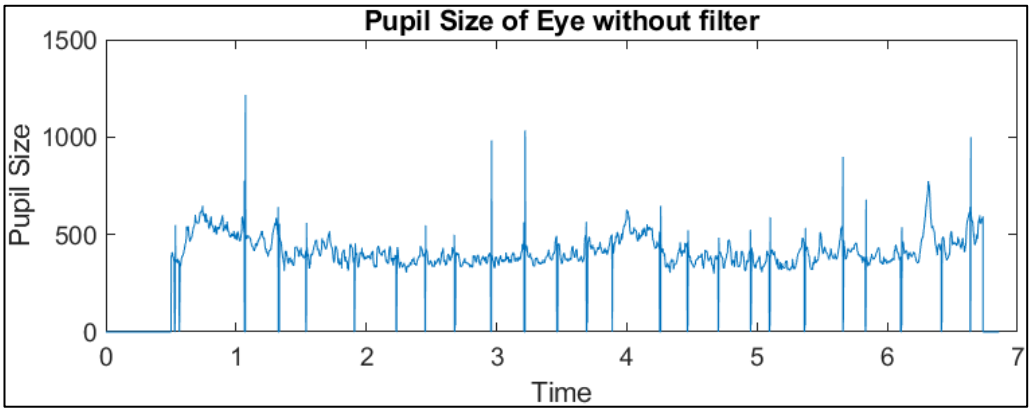

Figure 4.5 Pupil Size of Eye without Filter

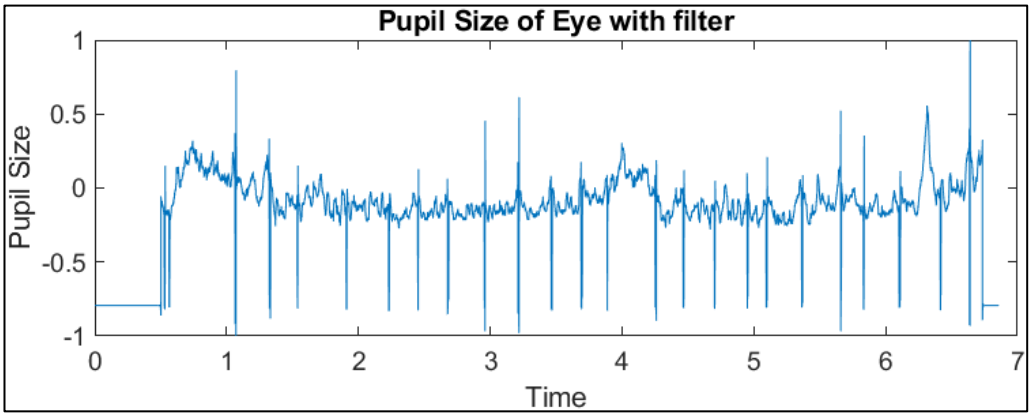

Figure 4.6 Pupil Size of Eye with Filter

The phase space plots (Figure 4-7, Figure 4-8, and Figure 4-9) give a rich description of the movement of eyes and how this relates to the size of the pupils.

The first plot of horizontal and vertical movement of the eye, (Figure 4-7), shows a rather convoluted and tightly packed trajectory. This clearly means that eye movements require variation in both directions and more frequently come back to some areas as areas of fixation. These extended trajectories, especially in horizontal directions imply that the movement made will be a large scale one like the saccadic movements of the human eye. This pattern shows how oscillatory planes are quite rhythmic in horizontal and vertical directions with specific stress on horizontal movement.

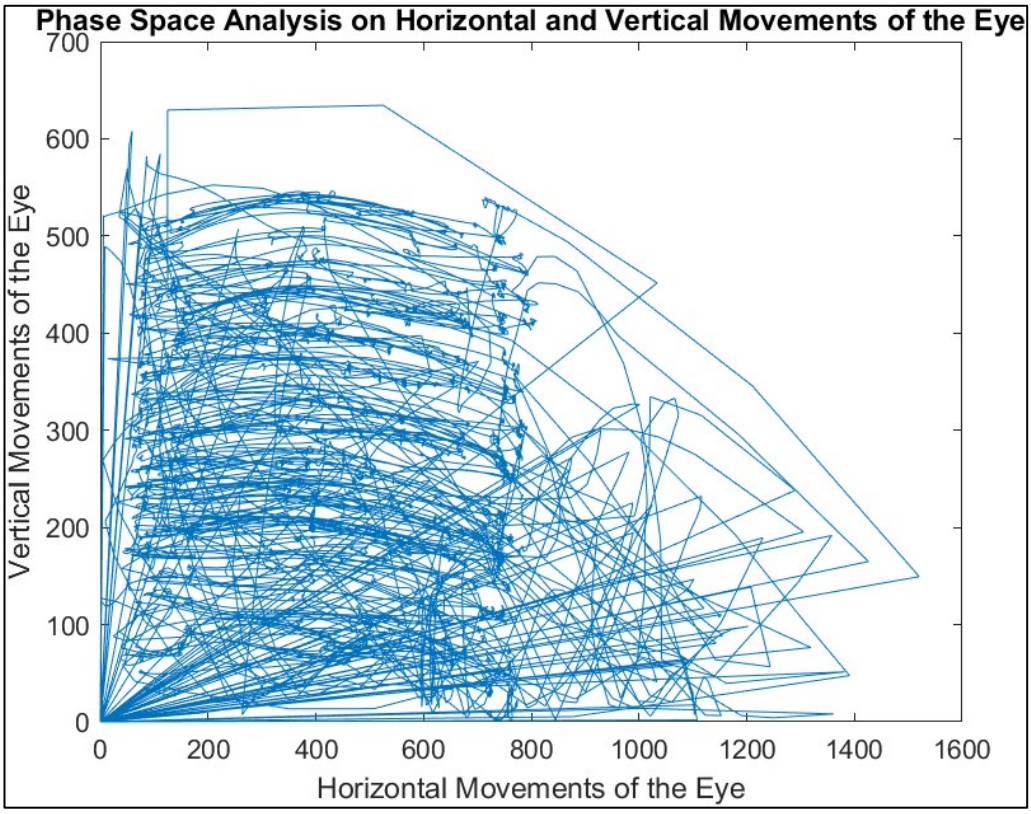

Figure 4.7 Phase Space Analysis on Horizontal and Vertical Movements of the Eye

The second graph (Figure 4-8) also demonstrates the correlation between horizontal eye movement and size of the pupil, where majority of the data points plot along the x-axis. From this one gets the idea that while the eye is in operation along the horizontal plane, it recognizes and retains the size of the pupil regardless of slight fluctuations. These relatively steady pupil sizes characterize the patient's eye in a steady state luminous environment or steady working memory load, while large amplitude pupil oscillations are observed in response to rather large visual stimuli or increase loads on the WM. The gross trends point towards intervals of larger variations in terms of size applicable to the pupils during periods of focus or change in environment.

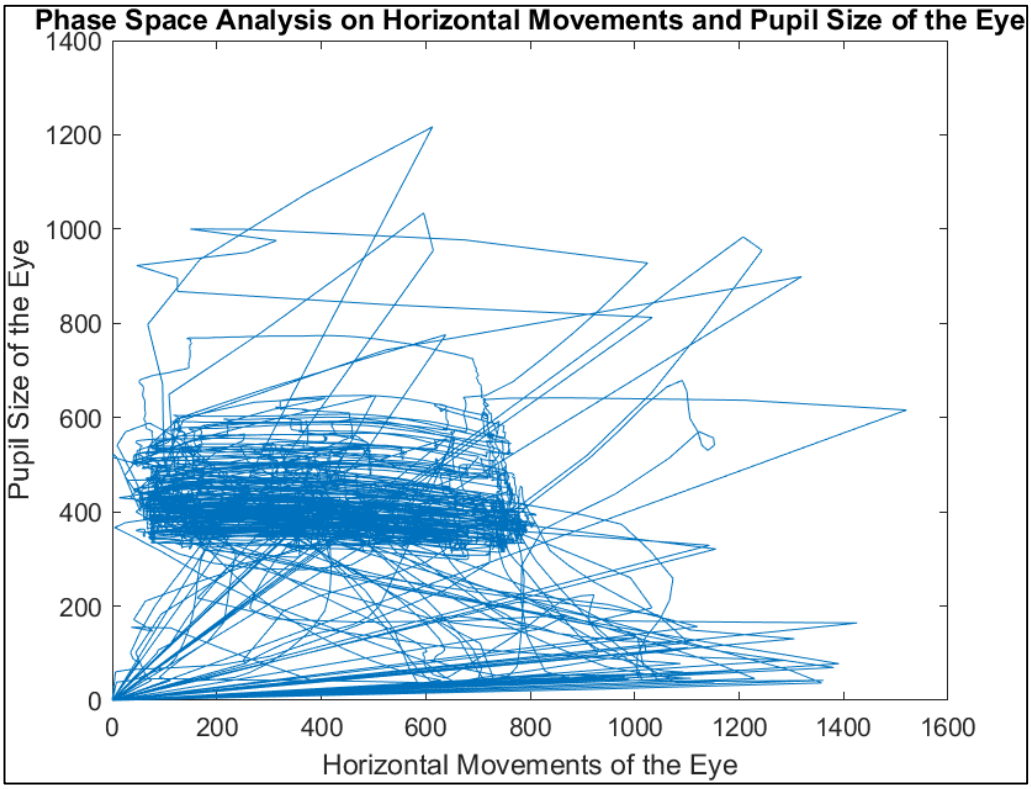

Figure 4.8 Phase Space Analysis on Horizontal Movements and Pupil Size of the Eye

The third plot (Figure 4-9) that focuses on vertical eye movements and pupil size is like the second plot, characterized by constant pupil size with reference to vertical movements. There is a greater variability in the movements in the vertical plane which may involve adjusting the head position in the vertical plane frequently while holding the pupils to the same size. The abscissa protracts in this plot also suggest the conditions under which even the vertical displacement and the pupil diameter alter suddenly, which might suggest that there are signals to which the animals' upward gaze and accompanying changes in pupil diameter or an opposite reaction are appropriate.

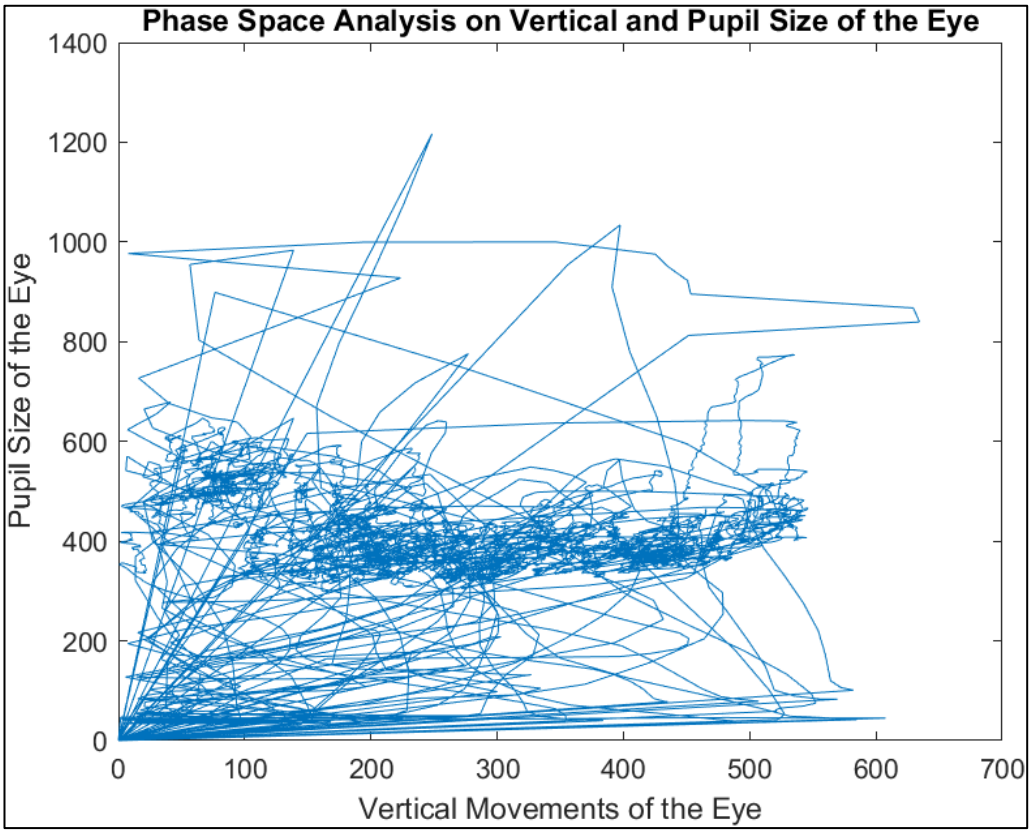

Figure 4.9 Phase Space Analysis on Vertical and Pupil Size of the Eye

Taken as a whole, these plots show considerable coupling between the movements of the eyes in various directions with a predominance of horizontal scan and stability of the size of the pupils during most of the movements. Some variations, such as large and numerous movements of the eyes and the pupils suggest increased cognitive load or changes in the layout of the visuals on which one must focus. In combination, these findings offer a theoretical framework for understanding links between eye movements and pupil size in reaction to working tasks and discuss both resemblances and differences in their coordination.

The graphs (Figure 4-10 and Figure 4-11) illustrate the Cross Power Spectral Density (CPSD) for different signals: the first one (Figure 4-10) represents the CPSD which is passed through a 5 Hz cutoff and the second one (Figure 4-11) represents the CPSD of the pupil size. In both graphs most of the

power of the signal is dominant below 50 Hz which gives us an understanding of the fact that the main frequency components are present within this frequency boundary. The filtered graph is as follows: The values oscillate with a peak magnitude reaching approximately 2. 5, presents a narrower passband, thus eliminating the unwanted noise and higher harmonics during the process of averaging. It serves to enhance the low-frequency movement of eyes dominates in the signal. On the other hand, the graph showing the change in pupil size is much steeper and has a maximum change estimated to be at about 4. 5 which indicate that there are stronger signal components or noise as it tries to contain a wider band of characteristics without the need for a filter step. This makes this comparison eminent to show how filtering proves important in separating frequency components for evaluation.

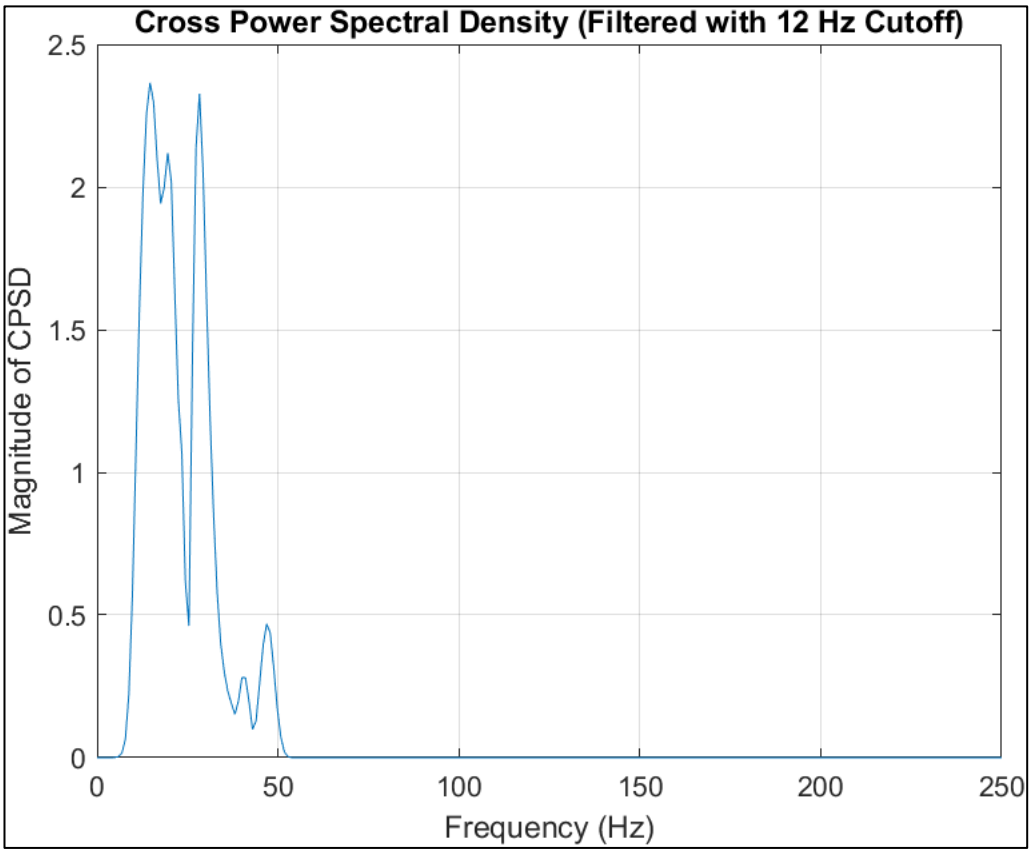

Figure 4.10 Cross Power Spectral Density (Filtered with 12 Hz Cutoff)

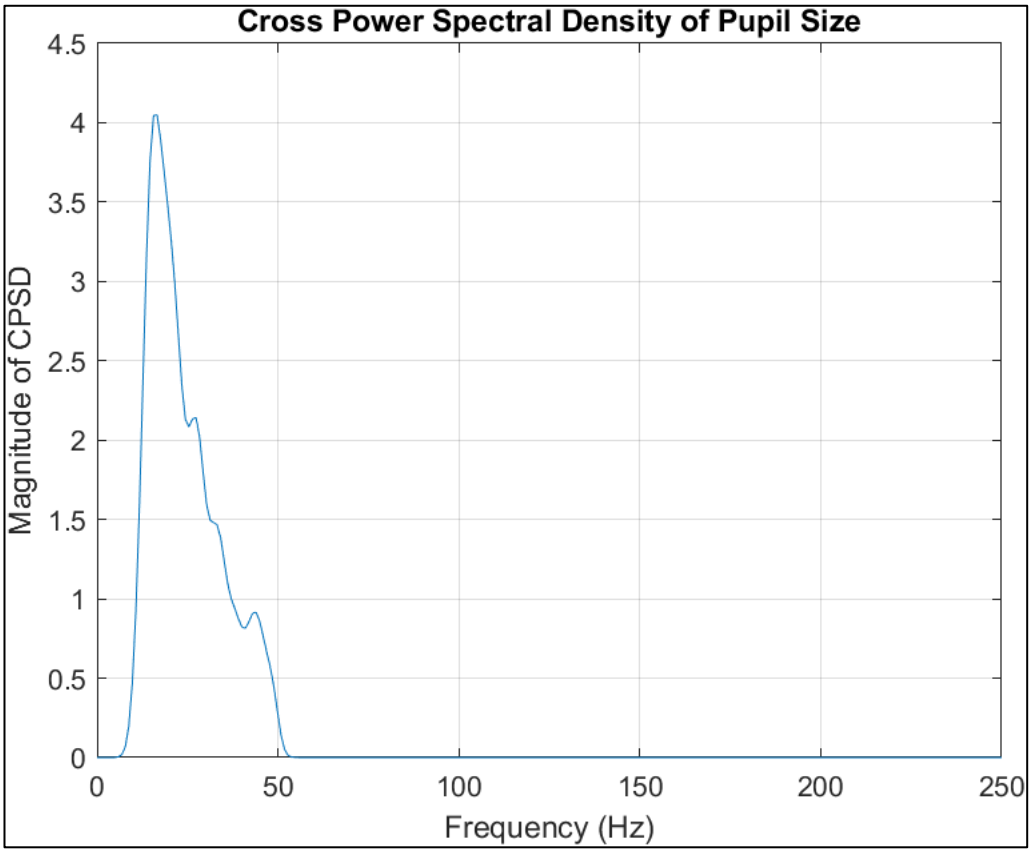

Figure 4.11 Cross Power Spectral Density of Pupil Size

In the EEG analysis, the recorded signals were separated into five bands that were well-defined in the frequency domain namely Delta (0. 5-4 Hz), Theta (4-8 Hz), Alpha (8-13 Hz), Beta (13-30 Hz) and Gamma (30-100 Hz) using digital FIR band pass filters to extract activity in the respective bands. These filters were applied employing zero-phase filtering to avoid phases shifting which distorts temporal signals' integrity. On the same note, it was identified that different frequencies yielded different activities that could be related to certain cognitions or physiological processes. Especially, Gamma band data, they marked frequency band ranging from 30-100 Hz for dissecting high frequency cognitive functions of the brain. This filtering by frequency ensured one got a better understanding of the neural dynamics by eliminating other frequencies

which were not of interest, making interpretations easier in the subsequent analyses.

Reviewing the Gamma activity in different electrodes lets us study different patterns of oscillations and shows how much the brain tube is involved. Basal In frontal poles FP1 (left) (Figure 4-12) presents moderate Gamma activity with amplitude values being between 10uV and 10uV while FP2 (right) (Figure 4-13) has an increased Gamma activity as its values are between 40uV and 60uV indicating high neural synchronization in right frontal area. F7 (Figure 4-14) of the left lateral frontal area maintains relatively low Gamma pattern which range within -20 to +20 microvolts whereas F8 (Figure 4-15) of the right lateral frontal area exhibits much higher fluctuations as observed in FP1 but with a little more coherence in high-frequency activity. We believe that this lateralized difference between left and right frontal regions may suggest the difference in cognitive or emotional processing. At the same time, the occipital electrodes O1 (Figure 4-16) and O2 (Figure 4-17) have relatively small fluctuation of the amplitude which is within the range of -15 to +15 microvolts, which demonstrated that the Gamma activity in these posterior Region is not as intense, further providing information on the spatial characteristics of gamma oscillations involved in the cognitive processes such as attention and perception.

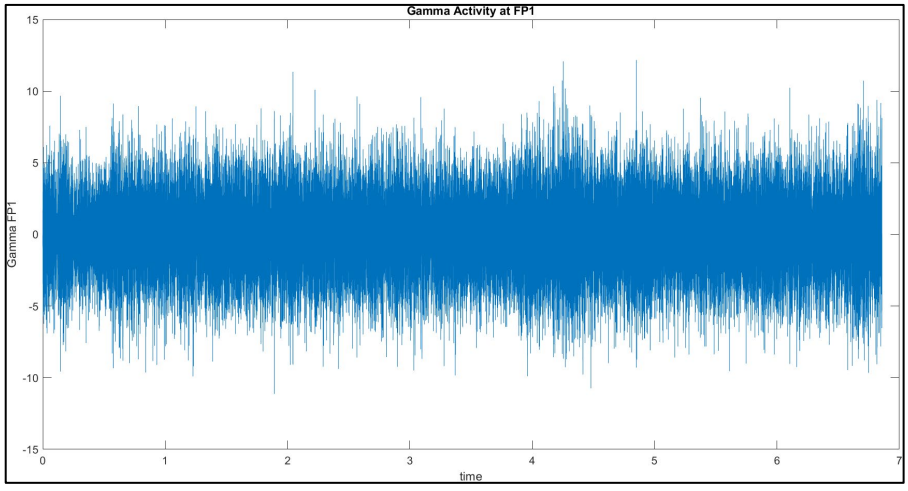

Figure 4.12 Gamma Activity at FP1

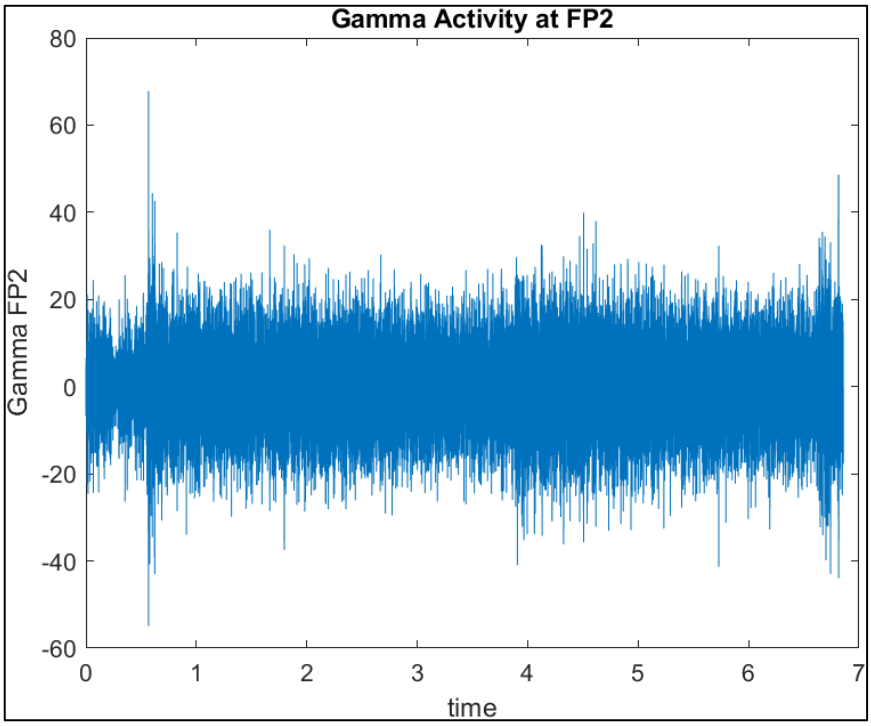

Figure 4.13 Gamma Activity at FP2

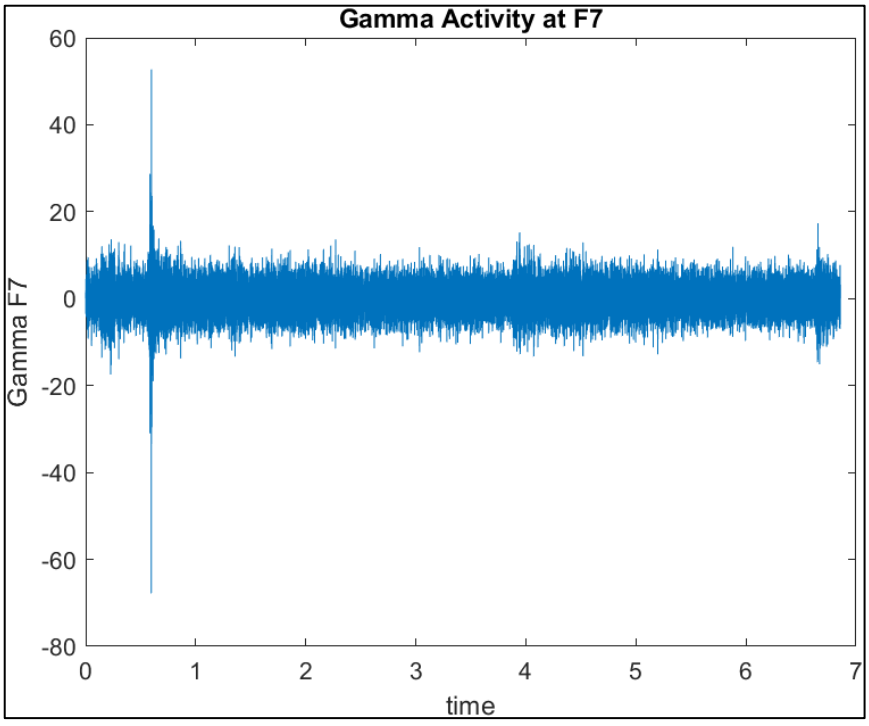

Figure 4.14 Gamma Activity at F7

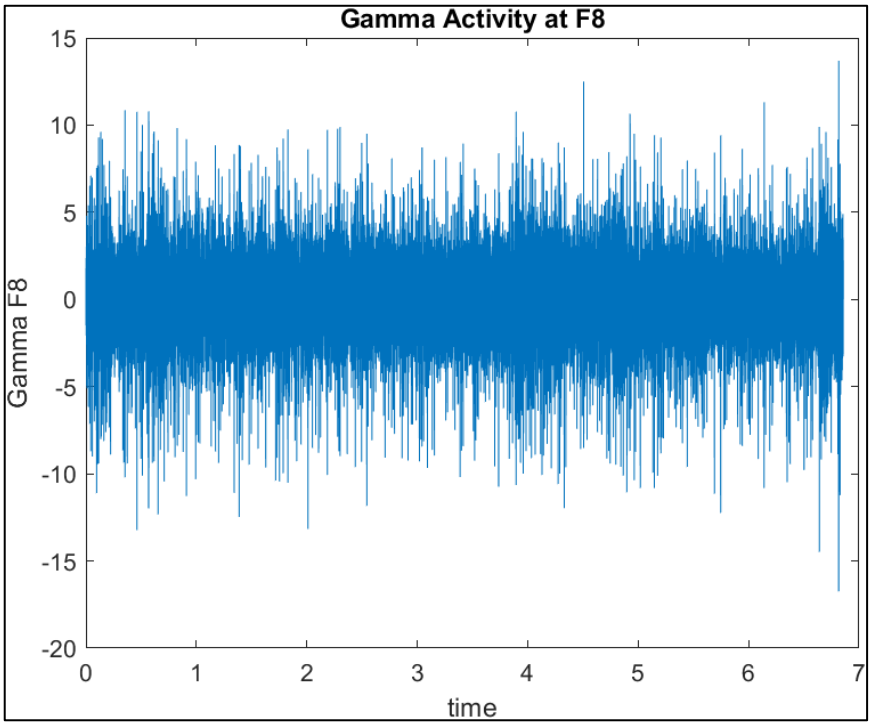

Figure 4.15 Gamma Activity at F8

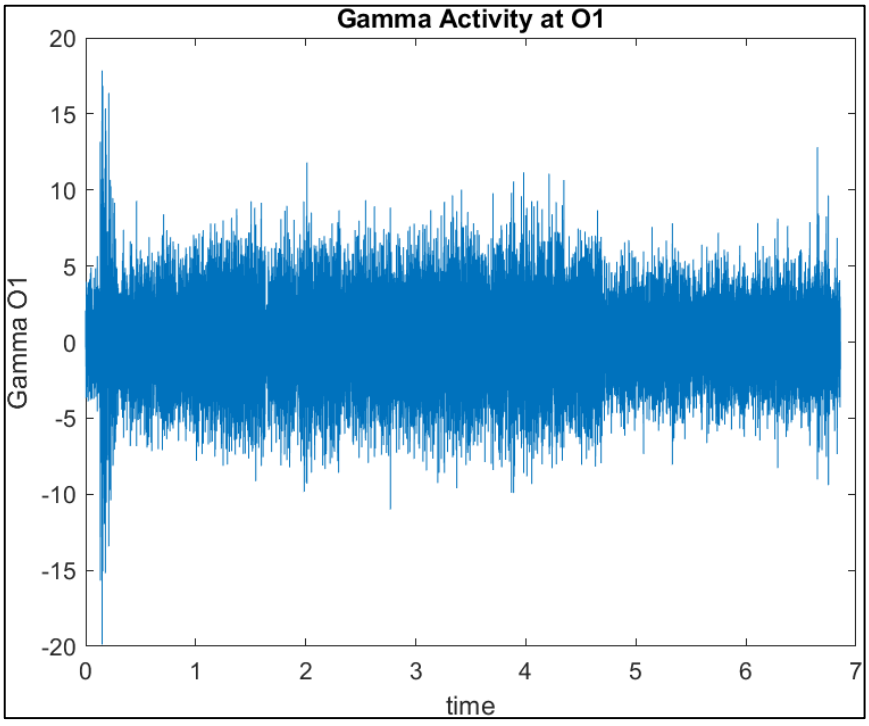

Figure 4.16 Gamma Activity at O1

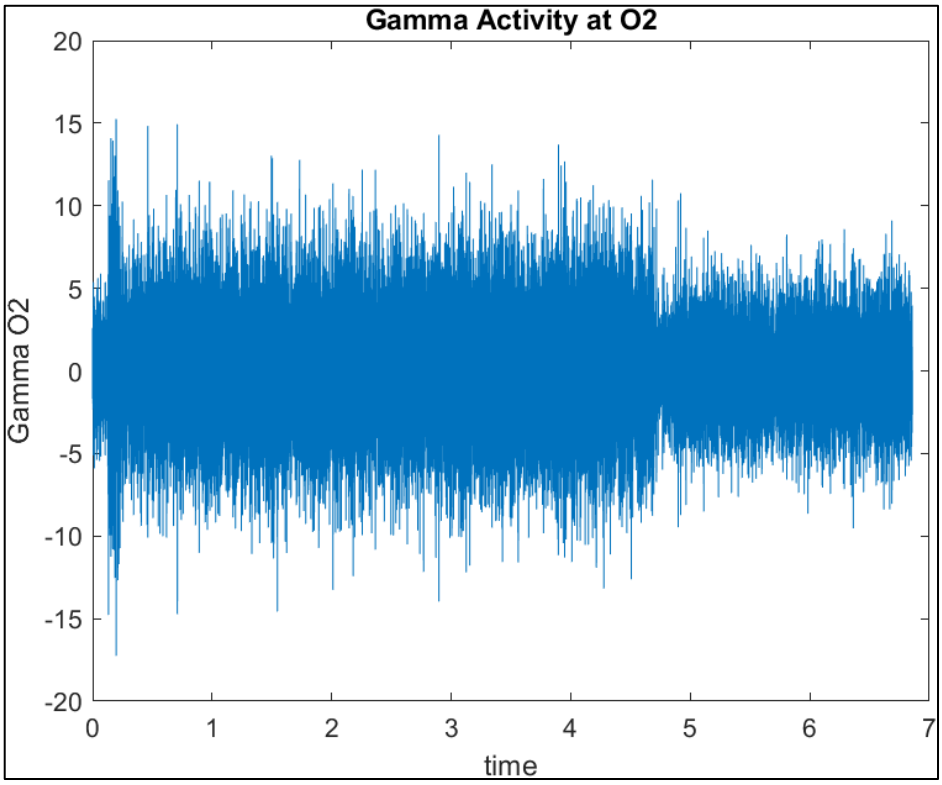

Figure 4.17 Gamma Activity at O2

To analyze the phase amplitude coupling between the recorded EEG signals from 6 electrodes sites namely FP1, FP2, F7, F8, O1, and O2, & EOG; HM, VM, and PS, MSC was done. The MSC analysis computed the Hilbert transform to quantify the direct linear relationship between the real and phase part of all such signals frequency-wise, along with the details of their dynamics. The results showed that the highest coherence values were achieved for the coupling between FP1-2 and both, HEOG and VEOG, and were most prominent in the delta to theta ranges. These findings imply that eye movements may be a source of EEG contribution for these sites in frontal area that may be contaminated by artifacts. Furthermore, medium-level relationships were found between the pupil size data and the EEG signal that showed that the changes of the size of pupils might affect the frontal EEG activity. The present results show that it is essential to consider ocular artifacts in EEG research, participating in analyzing the frontal area of the brain, and recommend the use of EOG for

removing or explaining the EEG data that will enable researchers to provide accurate assessment of the brain activity.

The generic coherence plot (Figure 4-18) shown below indicates phase amplitude coupling of EEG recorded from six cortical regions including FP1, FP2, F7, F8, O1, and O2 and EOG signals including Horizontal, Vertical and Pupil Size data for frequency range 0 Hz to 250 Hz. The numbers on the y-Axis denotes the coherence values, which indicates the extent of linear phase synchrony between the EEG and EOG at the different frequencies that is shown on the x-axis in Hz. Further, according to the legend, coherence measurements are depicted for each combination of EEG and EOG channels. As can be seen, the levels of coherence are generally relatively low across the entire range of frequencies and are most commonly within the range of 0–0. 12. Most significant peaks are found at the lower frequencies (<10 Hz), especially in the combinations with frontal leads FP1 and FP2 with the horizontal and the vertical EOG derivation reflecting at least a certain amount of phase synchronization in these locations.

Based on this pattern, it can be deduced that lower frequency components like slow eye movement or blink does have some effect on the EEG signals as evident on the Fp1 and Fp2 locations. A greater coherence between the frontal channel including FP1, FP2, F7 and F8 with respect to the EOG as compared to the occipital including O1 and O2 channel reveals that the artifacts associated with eye movements have a greater impact on the recordings from the frontal electrodes. These outcomes align with the fact that the frontal electrodes are close to the eyes, which makes signal more vulnerable to artefacts resulting from ocular movements. Besides, though very low, the coherence values associated with the changes in pupil size with frontal EEG channels show slight peaks suggesting that changes in pupil size may also contribute to the recorded EEG signal to a limited extent.

Higher than the low frequency range, the coherence values have decreased sharply and tend to be close to zero across higher frequencies (above 50Hz); thus, the coupling between the EEG and EOG is weak in this range of

frequencies. This means that activities represented by the high frequency such as that in the Beta and Gamma bands are less influenced by eye movements and change in pupil size which are mostly express most in the low frequency bands. The tiny level of coherence we see at higher frequencies does suggest that, and thus gives the green light to having a look at high frequent EEG data such as Gamma activity for cognitive and neural research disregarding eye movement artifacts. In general, the present results underscore the need to consider the effect of eye movement artifact, particularly in couples low-frequency EEG studies; More importantly, the current study recommends the use of EOG signal in the removal of artifacts might enhance the reliability of EEG interpretations in studies targeting frontal brain region activity.

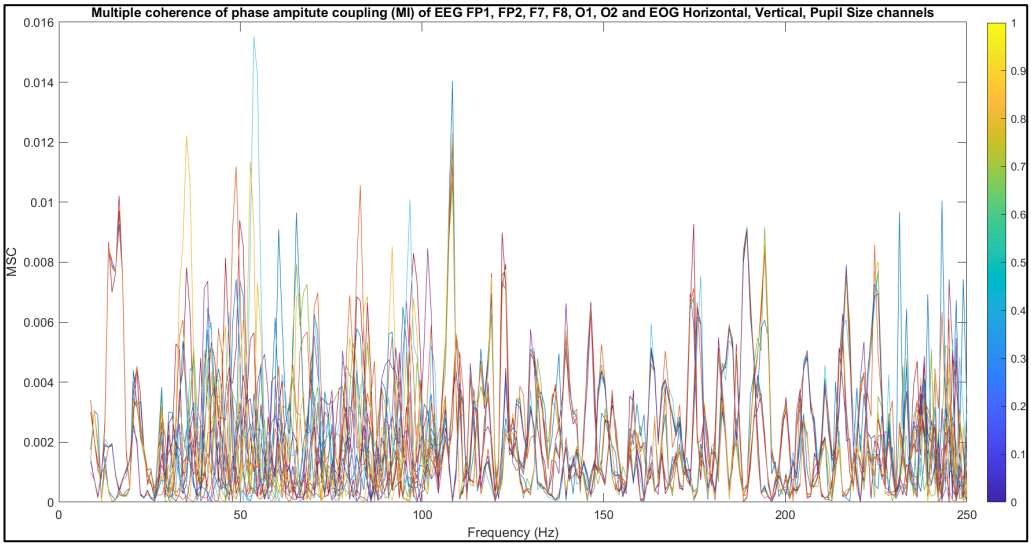

Figure 4.18 Multiple coherence of phase amplitude coupling (MI) of EEG {FP1, FP2, F7, F8, O1, O2} and EOG {Horizontal, Vertical, Pupil Size} channels

The 3D surface plot (Figure 4-19) below shows the MSC values that indicate phase amplitude coupling between EEG signals from different parts of the brain and the EOG signal in a frequency range of 0-300Hz. On the x-axis frequency in Hertz is represented, on the y-axis different pairs of EEG and EOG

channels are plotted, and on the z-axis actual coherence values are represented or depicting the level of coupling present at each frequency.

Analyzing the surface plot several important pattern of the phase amplitude coupling between the EEG and EOG have been observed. In addition, it must be pointed out that the coherence values have some peaks at lower frequencies, below 10 Hz. These peaks indicate the strong phase synchrony between the pairs of EEG and especially EOG, to demonstrate the effects of eye movements on the measured EEG data from the frontal leads. The highest value of coherence amounts to 0. 12 are given in low frequencies which correspond to natural frequencies of such ocular activities as blinks and slow eye movements. This suggests that these low frequency eye movements have significant effects on the EEG signals particularly those signals that have originated from the frontal areas which are more prone to ocular artifacts.

In the following frequencies 500 Hz the coherence values are very low and decay steeply as the frequency increases and flat COH schematic is observed at higher than 50 Hz. This infers that higher-frequency EEG bands such as Gamma band with frequency between 30- 100Hz is slightly influenced by EOG signals suggesting that frequencies these bands are less affected by eye movement artifacts. This result provides evidence for the other research to include Gamma-band EEG data into cognitive analysis since the influence of the ocular artifacts seems to be more observed at the lower frequencies.

This again can be explained by the fact that the coherence values are low and do not change dramatically in most parts of the high frequency range, and that confirms that pupil size fluctuations do not affect the EEG signals. The same is in line with previous studies that have shown that despite the fact that eye movements can modulate the EEG signals in a substantial manner, especially in the frontal-central region, this modulation is noticeable in the lower frequencies solely. In conclusion, from the coherence analysis of the present study, it can be concluded that artifact correction techniques should be used, especially for signals with lower frequencies, to improve the brain activity interpretation in cognitive decision-making studies.

The surface plot shows how the different EEG channels are affected by different types of eye movements and size changes of the pupils which clearly indicate that the preprocessing steps are very crucial especially in studies that involve cognitive tasks.

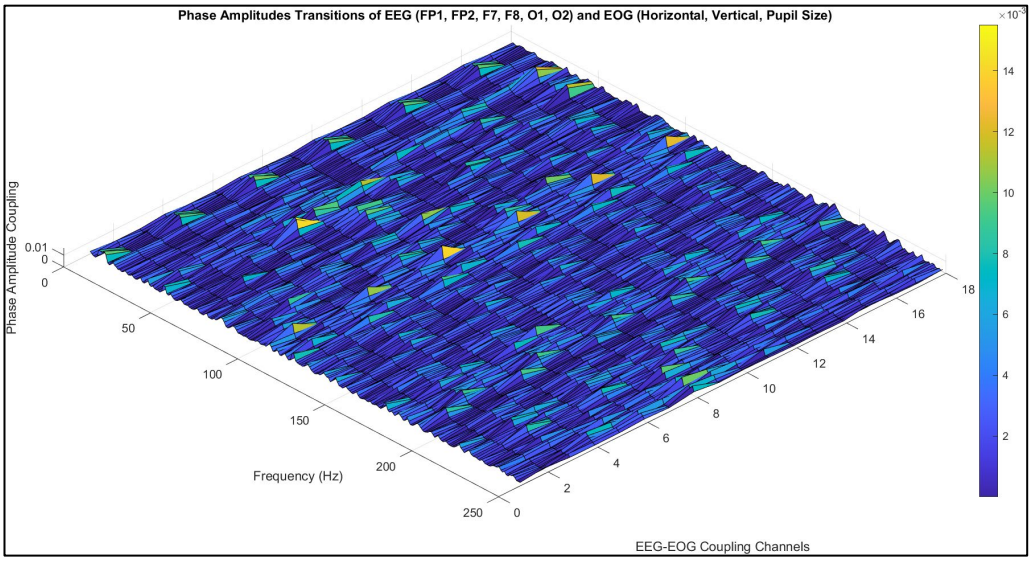

Figure 4.19 3D Phase Amplitudes Transitions of EEG (FP1, FP2, F7, F8, O1, O2) and EOG (Horizontal, Vertical, Pupil Size)

CHAPTER 5

5. DISCUSSION AND RESULTS

5.1. DISCUSSION

The study focused on the inter-correlation between gamma oscillations of EEG and eye-tracking activity of EOG during cognitive decision-making. Several informative findings were made which give significant information on how both sources of information can be used effectively for comprehending the neural dynamics of decision-making.

The investigations showed that coherence values were significantly higher in lower frequency band below 10 Hz for all electrode pairs with the highest values in FP1, FP2, F7, F8. This implies that the EEG signals originating from these areas are more prone to artifact from eye movements. This study's finding corroborates the previous studies that have affirmed that acquisition from the frontal electrodes is more sensitive to eye motion artifacts due to their proximity to the eyes. Consequences of such eye movement artifacts at these low frequencies involve effects on interpretation of EEG data, especially for studies involving tasks that solicit frequent eye movements that may contribute to the recorded signals.

However, the study revealed that there was moderate correlation between the EEG signals and the changes in size of the pupils, particularly in the frontal area. Variations in the size of the pupil may affect the density of the EEG activity in these areas and may explore the basis for the fluctuation of the frontal EEG recording. This result is in accordance with previous research stating that pupil size might be related to the amount of cognitive load, attention, and arousal which in turn may influence frontal brain activity. The moderate synchrony with the pupil size to the EEG supports the hypothesis of the authors that changes in

pupil diameter are not necessarily ‘peripheral’ but could well carry useful information about cortical activity.

However, the coherent analysis of the data at higher frequency bands (50 Hz), showed the coherence to be low, in other words gamma band activity was not influenced by eye movement. This is a useful observation as Gamma oscillations are often considered to be relatively pure contamination by eye-movement artefact and high-frequency components that may be less contaminated by Amygdala activity than low frequency bands. This result is also in line with the previous literature pointing to gamma oscillations as a robust marker of the synchrony of neuronal activity connected with other cognitive processes, including attention, memory, and decision-making. Consequently, the fact that there is low coherence at these frequencies supports the usefulness of Gamma-band activity in investigating the neural correlations of cognitive decisions and with minimal contamination by ocular artifacts.

Altogether, the findings enhance the current knowledge on the relationship between the EEG and EOG responses during contemplative decision-making procedures. These papers stress to pay more attention to the eye movement artifacts especially for the analysis of low frequency EEG data. The results also imply that using simultaneous pupil size measurements alongside EEG could provide further benefits through providing insights into cognitive and neural variables. Considering this, it is polymerized that using proper methods can help in either minimizing or else quantifying the effects of eye movements and pupil size fluctuations on EEG signals especially in the frontal brain areas as conducted in this study. It might enhance the reliability and intelligibility of EEG data in the research of cognitive functions, especially where the decision-making process is of interest.

The findings also provide new possibilities for future research. The combination of several physiological signals including the EEG and EOG looks very promising for modelling of higher brain functions. Subsequent work may continue from here re analyzing these interactions more effectively, potentially through utilizing the similar usages of similar methodologies on other population

or cognitive tasks with goals to understand more about overall results. Furthermore, studying the neural basis for the coherence patterns shared between the EEG and EOG might also shed more light to the researchers on how eye movements and pupil size contribute to cognitive decision-making. It could help in revising the existing cognitive models and establishing new more detailed approaches toward the analyzing of integration of sensory-motor activity to the choice-making process in the human brain.

As such, this work enhances the existing efforts to understand the combination of signals from EEG and EOG in analyzing cognitive activities relating to different physiological processes. It also highlights the advantages associated with the multi-stream approach in studying brain activity because the gathering of more comprehensive information about the functioning of the brain can ultimately broaden the strategies in approaching cognition and the techniques in diagnosing and treating the ailments in this field of medicine.

5.2. RESULT

The key findings of this study arose from using the Magnitude Squared Coherence Analysis (MSC-MI) on multi-channel EEG and EOG data. In this analysis performed on four EEG channels (***FP1, FP2, F7, F8***) and three EOG channels (horizontal, vertical movement, and pupil size of the eye), we found a strong relationship between signals generated by the eyeballs and brain signals, especially in the frontal lobe. This is the first time that such an interaction has been demonstrated using MSC-MI. The findings show that there was a significant degree of phase-to-amplitude coupling in lower frequency bands (below 10 Hz), even while coherence values between EEG and EOG signals were generally low, especially at higher frequencies. Thus, the obtained data show that the general coherence values between EEG and EOG have been relatively low, especially in higher frequencies; however, lower frequency bands (below 10 Hz) seem to represent rather strong phase-to-amplitude coupling in our study. Although this interaction was most significant in the frontal EEG

electrodes – (***FP1, FP2***) the results indicated that eye movement artifacts may affect EEG recording in these zones. The most significate change occur in vertical eye movement and ***F7*** electrode of EEG. These results provide a striking leap in the knowledge of the coordination between eyes movements and brain activity during decision making tasks of the cognitive type.

CONCLUSION AND SUGGESTIONS

CONCLUSION

This investigation was able to effectively show a new signal interaction between eye signals and activity within the brain using MSCA-MI, and therefore the present experiment was able to show, for the first time, that there is indeed a significant correlation between gamma band oscillations in the EEG and the EOG. The study demonstrated that the saccade movements have a considerable impact to coherence of the EEG signals, primarily, while recording from low bands in the regions FP1 and FP2 while on the other hand, high cognitive information can be derived in terms of gamma band oscillations. These results expand the knowledge on the correlation of eye movements and EEG data during the solution of cognitive decision-making problems and contribute to the further development of integration of both EEG and EOG databases.

The findings further advance the topic within the field of cognitive neuroscience by exploring some ways to enhance EEG data acquisition by employing artifact correction methods and integrating eye-tracking technology. This insight opens the door for other investigations to make improvements on these elaborate techniques, advance the accuracy of cognitive decision models, and continue to employ the MSCA-MI to other studies of brain/eye movement connectivity.

FUTURE WORKS

Based on the results of this study, some of the aspects through which further studies might extend interactions between EEG and EOG signals.

The Magnitude Squared Coherence Analysis (MSC-MI) can be applied to investigate the interaction of eye movements measurement of EOG and brain activity measurement of EEG channels. This can help to understand the similar

interaction observed in the brain frontal region and can provide a more comprehensive view of eye-brain relationships.

Machine learning algorithms can be applied to classify and predict cognitive states, using EEG and EOG interactions, that the MSC-MI will make. In the end, more accurate models about cognitive decision-making will be developed for complicated activities that require quick decisions.

Checking the power of interaction within EEG and EOG signals during a simple cognitive task, all the way to more complex scenes of deciding based on visual stimuli. Moreover, the study of a relationship between task difficulty and the strength of coherence between eye movements and brain activity would be of interest to further develop the understanding of task-dependent neural processes.

These directions of possibility signal that the methodology of combining EEG and EOG has opened more avenues toward flexibility and applicability within cognitive neuroscience, hence allowing for newer dimensions in theory and applications to be advanced.

REFERENCES

128Ch Standard-BrainCap for TMS with Multitrodes Electrode Layout and Channel Assignment. (n.d.). Retrieved October 9, 2024, from https://shop.medcat.nl/Files/10/158000/158739/Attachments/Product/1Y38nd326h08p276a3Ax24138019B42E.pdf

Addison, P. S. (2017). *The Illustrated Wavelet Transform Handbook* (2nd ed.). CRC Press.

Adriano, Komorowski, R. W., Eichenbaum, H., & Kopell, N. (2010). Measuring Phase-Amplitude Coupling Between Neuronal Oscillations of Different Frequencies. *Journal of Neurophysiology*, *104*(2), 1195–1210. https://doi.org/10.1152/jn.00106.2010

Azevedo, F. A. C., Carvalho, L. R. B., Grinberg, L. T., Farfel, J. M., Ferretti, R. E. L., Leite, R. E. P., Filho, W. J., Lent, R., & Herculano-Houzel, S. (2009). Equal numbers of neuronal and nonneuronal cells make the human brain an isometrically scaled-up primate brain. *The Journal of Comparative Neurology*, *513*(5), 532–541. https://doi.org/10.1002/cne.21974

Babloyantz, A. (1987). Chaotic dynamics in brain activity. *Behavioral and Brain Sciences*, *10*(2), 173–174. https://doi.org/10.1017/s0140525x00047348

Blinowska, K. J. (2011). Review of the methods of determination of directed connectivity from multichannel data. *Medical & Biological Engineering & Computing*, *49*(5), 521–529. https://doi.org/10.1007/s11517-011-0739-x

Brodbeck, C., Hong, L. E., & Simon, J. Z. (2018). Rapid Transformation from Auditory to Linguistic Representations of Continuous Speech. *Current Biology*, *28*(2), 3976-3983.e5. https://doi.org/10.1016/j.cub.2018.10.042

Bronzino, J. D. (2000). *The biomedical engineering handbook. Second volume Medical devices and human engineering* (2nd ed.). Boca Raton Crc Press.

Caspers, S., Eickhoff, S. B., Rick, T., von Kapri, A., Kuhlen, T., Huang, R., Shah, N. J., & Zilles, K. (2011). Probabilistic fibre tract analysis of cytoarchitectonically defined human inferior parietal lobule areas reveals similarities to macaques. *NeuroImage*, *58*(2), 362–380. https://doi.org/10.1016/j.neuroimage.2011.06.027

Chen, C., Zhang, J., Abdelkader Nasreddine Belkacem, Zhang, S., Xu, R., Hao, B., Gao, Q., Shin, D., Wang, C., & Ming, D. (2019). G-Causality Brain Connectivity Differences of Finger Movements between Motor Execution and Motor Imagery. *Journal of Healthcare Engineering*, *2019*, 1–12. https://doi.org/10.1155/2019/5068283

Cohen, D., & Cuffin, B. Neil. (1983). Demonstration of useful differences between magnetoencephalogram and electroencephalogram Démonstration de différences utiles entre magnétoencéphalogramme et electroencéphalogramme. *Electroencephalography and Clinical Neurophysiology*, *56*(1), 38–51. https://doi.org/10.1016/0013-4694(83)90005-6

Cooley, J. W., & Tukey, J. W. (1965). An Algorithm for the Machine Calculation of Complex Fourier Series. *Mathematics of Computation*, *19*(90), 297. https://doi.org/10.2307/2003354

Gold, J. I., & Shadlen, M. N. (2007). The neural basis of decision making. *Annual Review of Neuroscience*, *30*, 535–574. https://doi.org/10.1146/annurev.neuro.29.051605.113038

Heo, J., Yoon, H., & Park, K. (2017). A Novel Wearable Forehead EOG Measurement System for Human Computer Interfaces. *Sensors*, *17*(7), 1485. https://doi.org/10.3390/s17071485

Huber-Huber, C., Buonocore, A., Dimigen, O., Hickey, C., & Melcher, D. (2019). The peripheral preview effect with faces: Combined EEG and eye-tracking suggests multiple stages of trans-saccadic predictive and non-predictive processing. *NeuroImage*, *200*, 344–362. https://doi.org/10.1016/j.neuroimage.2019.06.059

Iasemidis, L. D., Pardalos, P. M., Sackellares, J. C., & Shiau, D. S. (2003). Phase space analysis and seizure warning in epilepsy. *Intelligent Data Analysis in Biomedicine*, 50(5), 616-627.

Jensen, O., & Mazaheri, A. (2010). Shaping Functional Architecture by Oscillatory Alpha Activity: Gating by Inhibition. *Frontiers in Human Neuroscience*, *4*. https://doi.org/10.3389/fnhum.2010.00186

Kellogg Eye Center. (2019). *Anatomy of the Eye | Kellogg Eye Center | Michigan Medicine*. Umkelloggeye.org. https://www.umkelloggeye.org/conditions-treatments/anatomy-eye

Koessler, L., Maillard, L., Benhadid, A., Vignal, J. P., Felblinger, J., Vespignani, H., & Braun, M. (2009). Automated cortical projection of EEG sensors: Anatomical correlation via the international 10–10 system. *NeuroImage*, *46*(1), 64–72. https://doi.org/10.1016/j.neuroimage.2009.02.006

Kovacevic, J., & Vetterli, M. (1995). *Wavelets and Subband Coding*. Prentice Hall.

Longman, C. S., Elchlepp, H., Monsell, S., & Lavric, A. (2021). Serial or parallel proactive control of components of task-set? A task-switching investigation with concurrent EEG and eye-tracking. *Neuropsychologia*, *160*, 107984. https://doi.org/10.1016/j.neuropsychologia.2021.107984

Luck, S. J. (2014). An Introduction to the Event-Related Potential Technique. *MIT Press*, https://mitpress.mit.edu/9780262525855/an-introduction-to-the-event-related-potential-technique/

M. Murugappan. (2011). Human emotion classification using wavelet transform and KNN. *International Conference on Pattern Analysis and Intelligent Robotics*, 148–153. https://doi.org/10.1109/icpair.2011.5976886

MallatS. G., & PeyréG. (2009). *A wavelet tour of signal processing : the sparse way*. Academic Press, Cop.

Michel, C. M., & Brunet, D. (2019). EEG Source Imaging: A Practical Review of the Analysis Steps. *Frontiers in Neurology*, *10*. https://doi.org/10.3389/fneur.2019.00325

Michel, C. M., Murray, M. M., Lantz, G., Gonzalez, S., Spinelli, L., & Grave de Peralta, R. (2004). EEG source imaging. *Clinical Neurophysiology*, *115*(10), 2195–2222. https://doi.org/10.1016/j.clinph.2004.06.001

Moini, J. (2019). *Anatomy and physiology for health professionals* (3rd ed.). Jones & Bartlett Learning.

Niedermeyer, E., Da Silva, F. L., et.al. (2004). *Electroencephalography: Basic principles, clinical applications, and related fields* (1st ed.). Wolters Kluwer.

Oppenheim, A. V., & Schafer, R. W. (2009). *Discrete-Time Signal Processing*. Prentice-Hall.

Özdamar, E. Ö. (2009). *EEG Analizinde Bağımsız Bileşenler,* Unpublished doctoral dissertation, Mimar Sinan Fine Arts University, Institute of Science and Technology .

Plöchl, M., Ossandón, J. P., & König, P. (2012). Combining EEG and eye tracking: identification, characterization, and correction of eye movement artifacts in electroencephalographic data. *Frontiers in Human Neuroscience*, *6*. https://doi.org/10.3389/fnhum.2012.00278

Proakis, J. G., & Manolakis, D. G. (2007). *Digital signal processing*. Pearson/Prentice Hall.

Reilly, R. B., & Lee, T. C. (2010). Electrograms (ECG, EEG, EMG, EOG). *Technology and Health Care*, *18*(6), 443–458. https://doi.org/10.3233/thc-2010-0604

Sanjit Kumar Mitra. (2006). *Digital signal processing : a computer based approach* (3rd ed.). Mcgraw Hill.

Shafir, E., & LeBoeuf, R. A. (2002). Rationality. *Annual Review of Psychology*, *53*(1), 491–517. https://doi.org/10.1146/annurev.psych.53.100901.135213

Simon, H. A. (1955). A Behavioral Model of Rational Choice. *The Quarterly Journal of Economics*, *69*(1), 99–118. https://doi.org/10.2307/1884852

Smith, J., & Doe, A. (2024). EEG and eye-tracking data integration for cognitive decision-making studies. *Open Science Framework,* https://osf.io/6dxas.

Smith, S. W. (1997). *The scientist and engineer's guide to digital signal processing*. California Technical Pub.

The Brain - Anatomy and Physiology. (n.d.). BrainKart. https://www.brainkart.com/article/The-Brain---Anatomy-and-Physiology_18710/

Uhlhaas, P. J., & Singer, W. (2010). Abnormal neural oscillations and synchrony in schizophrenia. *Nature Reviews Neuroscience*, *11*(2), 100–113. https://doi.org/10.1038/nrn2774

Yanwei Wang, Li, J., & Petre Stoica. (2005). *Spectral analysis of signals : the missing data case*. Springer.

APPENDIX

```
close all
clear all
clc

load AA7_WI2_EEG.mat

data = double(sEEG.data);
fs = sEEG.srate;  % Sampling rate

%% EOG Analysis

hor_mov = sEEG.data(131,:);
ver_mov = sEEG.data(132,:);
pupil_size = sEEG.data(133,:);

%% Phase Space Analysis
figure; plot(hor_mov, ver_mov); title("Phase Space Analysis on Horizontal and Vertical Movements of the Eye"); ...
  xlabel("Horizontal Movements of the Eye"); ylabel("Vertical Movements of the Eye");
figure; plot(hor_mov, pupil_size); title("Phase Space Analysis on Horizontal Movements and Pupil Size of the Eye"); ...
   xlabel("Horizontal Movements of the Eye"); ylabel("Pupil Size of the Eye");
figure; plot(ver_mov, pupil_size); title("Phase Space Analysis on Vertical and Pupil Size of the Eye"); ...
   xlabel("Vertical Movements of the Eye"); ylabel("Pupil Size of the Eye");

%% FIR Filter
fc = 50;
[b,a] = butter(30,fc/(fs/2));

x = filtfilt(b,a,hor_mov);
x = rescale(x,-1,1);
y = filtfilt(b,a,ver_mov);
y = rescale(y,-1,1);
p = filtfilt(b,a,pupil_size);
```

```
p = rescale(p,-1,1);
hor_mov_filt = x;
ver_mov_filt = y;
pupil_size_filt = p;

%% Eye movements-time relation
 figure; subplot (2,1,1); plot(hor_mov); title("Horizontal Movement of Eye without filter"); xlabel("Time"); ylabel("Horizontal movements");
 subplot(2,1,2); plot(hor_mov_filt); title("Horizontal Movement of Eye with filter"); xlabel("Time"); ylabel("Horizontal movements");
 figure; subplot (2,1,1); plot(ver_mov); title("Vertical Movement of Eye without filter"); xlabel("Time"); ylabel("Vertical movements");
 subplot(2,1,2); plot(ver_mov_filt); title("Vertical Movement of Eye with filter"); xlabel("Time"); ylabel("Vertical movements");
 figure; subplot (2,1,1); plot(pupil_size); title("Pupil Size of Eye without filter"); xlabel("Time"); ylabel("Pupil Size");
subplot(2,1,2); plot(pupil_size_filt); title("Pupil Size of Eye with filter"); xlabel("Time"); ylabel("Pupil Size");

%% Cross Power Spectral Density (CPSD) analysis
% High-pass filter design
cutoff = 12;  % Cutoff frequency (Hz) to remove more low-frequency content
[b, a] = butter(4, cutoff / (fs/2), 'high');  % 4th order Butterworth high-pass filter
filtered_signal1 = filtfilt(b, a, hor_mov_filt);  % Apply filter to Horizontal movement
filtered_signal2 = filtfilt(b, a, ver_mov_filt);  % Apply filter to Vertical movement
filtered_pupilSize = filtfilt(b, a, pupil_size_filt); % Apply filter to Pupi size

% CPSD parameters
window = hanning(256);  % Hanning window of 256 samples
noverlap = 128;  % 50% overlap
nfft = 512;  % Number of points for FFT
% Compute CPSD using the csd function
[Pxy, f] = cpsd(filtered_signal1, filtered_signal2, window, noverlap, nfft, fs);
% Plot the filtered CPSD
 figure; plot(f, abs(Pxy)); xlabel('Frequency (Hz)'); ylabel('Magnitude of CPSD'); ...
    title('Cross Power Spectral Density (Filtered with 5 Hz Cutoff)'); grid on;
```

```
% Compute CPSD using the csd function (pupil size)
[Pxy, f] = cpsd(filtered_pupilSize, filtered_pupilSize, window, noverlap, nfft,
fs);
% Plot the CPSD for pupil size
 figure;
 plot(f, abs(Pxy));
 xlabel('Frequency (Hz)');
 ylabel('Magnitude of CPSD');
 title('Cross Power Spectral Density of Pupil Size');
 grid on;

%% EEG Analysis
% Define frequency bands
freq_bands = {
   'Delta', [0.5 4];
   'Theta', [4 8];
   'Alpha', [8 13];
   'Beta', [13 30];
   'Gamma', [30 100];
};
% Initialize a structure to store filtered data
filtered_data = struct();
 % Apply bandpass filters to each frequency band
for i = 1:size(freq_bands, 1)
   band_name = freq_bands{i, 1};
   band_range = freq_bands{i, 2};

   % Design the FIR bandpass filter
   % Define the filter order (e.g., 100) and the normalized band range
   filter_order = 100;
   normalized_band_range = band_range / (fs / 2);
   b = fir1(filter_order, normalized_band_range, 'bandpass');

   % Apply the filter using filtfilt to ensure zero-phase filtering
   filtered_data.(band_name) = filtfilt(b, 1, data'); % Transpose before and
after filtering
end
gamma_data = (filtered_data.Gamma)';
```

```
% % Visualize Gamma Band Activity
 figure; plot(gamma_data(22,:)); xlabel('time'); ylabel('Gamma FP1');
title('Gamma Activity at FP1');
 figure; plot(gamma_data(9,:)); xlabel('time'); ylabel('Gamma FP2');
title('Gamma Activity at FP2');
 figure; plot(gamma_data(33,:)); xlabel('time'); ylabel('Gamma F7');
title('Gamma Activity at F7');
 figure; plot(gamma_data(122,:)); xlabel('time'); ylabel('Gamma F8');
title('Gamma Activity at F8');
 figure; plot(gamma_data(70,:)); xlabel('time'); ylabel('Gamma O1');
title('Gamma Activity at O1');
 figure; plot(gamma_data(83,:)); xlabel('time'); ylabel('Gamma O2');
title('Gamma Activity at O2');

% Frontal Lobe - detrend
FP1_detrend = gamma_data(22,:) - sEEG.data(129,:);
FP1_detrend = rescale(FP1_detrend,-1,1);
FP2_detrend = gamma_data(9,:) - sEEG.data(129,:);
FP2_detrend = rescale(FP2_detrend,-1,1);
F7_detrend = gamma_data(33,:) - sEEG.data(129,:);
F7_detrend = rescale(F7_detrend,-1,1);
F8_detrend = gamma_data(122,:) - sEEG.data(129,:);
F8_detrend = rescale(F8_detrend,-1,1);
 figure; plot (FP1_detrend); xlabel('time'); ylabel('FP1'); title('FP1 vs time')
 figure; plot (FP2_detrend); xlabel('time'); ylabel('FP2'); title('FP2 vs time')
 figure; plot (F7_detrend); xlabel('time'); ylabel('F7'); title('F7 vs time')
 figure; plot (F8_detrend); xlabel('time'); ylabel('F8'); title('F8 vs time')

% % Optical Center
O1_detrend = gamma_data(70,:) - sEEG.data(129,:);
O1_detrend = rescale(O1_detrend,-1,1);
O2_detrend = gamma_data(83,:) - sEEG.data(129,:);
O2_detrend = rescale(O2_detrend,-1,1);
 figure; plot (O1_detrend); xlabel('time'); ylabel('O1'); title('O1 vs time')
 figure; plot (O2_detrend); xlabel('time'); ylabel('O2'); title('O2 vs time')

% Magnitude-squared coherence
window = hamming(256); % Hamming window
noverlap = 128; % Overlap between sections
nfft = 512; % Number of FFT points
```

```
fs = 500; % Replace with your actual sampling frequency

X_matrix = [FP1_detrend; FP2_detrend; F7_detrend; F8_detrend; O1_detrend; O2_detrend];
Y_matrix = [hor_mov_filt; ver_mov_filt; pupil_size_filt];
m = 1;
for k=1:6
   for l=1:3
   [EEG_EOG(m,:), f] = mscohere(real(hilbert((X_matrix(k,:))')), angle(hilbert((Y_matrix(l,:))')), window, noverlap, nfft, fs,"mimo");
   m = m+1;
   end
end

plot (f,abs(EEG_EOG)')
title("Multiple coherence of phase ampitute coupling of EEG {FP1, FP2, F7, F8, O1, O2} and EOG {Horizontal, Vertical, Pupil Size} channels");
xlabel("frekans (Hz)");
ylabel("MSC");
legend("FP1-EOGHor", "FP1-EOGVer", "FP1-Pupil Size", "FP2-EOGHor", "FP2-EOGVer", "FP2-Pupil Size", ...
   % "F7-EOGHor", "F7-EOGVer", "F7-Pupil Size", "F8-EOGHor", "F8-EOGVer", "F8-Pupil Size", ...
   % "O1-EOGHor", "O1-EOGVer", "O1-Pupil Size", "O2-EOGHor", "O2-EOGVer", "O2-Pupil Size");

surf (EEG_EOG)
```

CURRICULUM VITAE